Diurnal variation of stratospheric and lower mesospheric HOCl, ClO and HO2 at the equator: comparison of 1-D model calculations with measurements by satellite instruments

Atmos. Chem. Phys., 13, 7587–7606, 2013
www.atmos-chem-phys.net/13/7587/2013/
doi:10.5194/acp-13-7587-2013

Atmospheric Chemistry and Physics Open Access

Diurnal variation of stratospheric and lower mesospheric HOCl, ClO and HO_2 at the equator: comparison of 1-D model calculations with measurements by satellite instruments

M. Khosravi[1], P. Baron[2], J. Urban[1], L. Froidevaux[3], A. I. Jonsson[4], Y. Kasai[2,5], K. Kuribayashi[2,5], C. Mitsuda[6], D. P. Murtagh[1], H. Sagawa[2], M. L. Santee[3], T. O. Sato[2,5], M. Shiotani[7], M. Suzuki[8], T. von Clarmann[9], K. A. Walker[4], and S. Wang[3]

[1]Department of Earth and Space Sciences, Chalmers University of Technology, Gothenburg, Sweden
[2]National Institute of Information and Communications Technology, Tokyo, Japan
[3]Jet Propulsion Laboratory, California Institute of Technology, Pasadena, CA, USA
[4]Department of Physics, University of Toronto, Toronto, Ontario, Canada
[5]Tokyo Institute of Technology, Yokohama, Kanagawa, Japan
[6]Fujitsu FIP Corporation, Tokyo, Japan
[7]Research Institute for Sustainable Humanosphere, Kyoto University, Kyoto, Japan
[8]Institute of Space and Astronautical Science, Japan Aerospace Exploration Agency, Sagamihara, Kanagawa, Japan
[9]Karlsruhe Institute of Technology, Institute for Meteorology and Climate Research, Karlsruhe, Germany

Correspondence to: M. Khosravi (maryam.khosravi@chalmers.se)

Received: 10 May 2012 – Published in Atmos. Chem. Phys. Discuss.: 20 August 2012
Revised: 29 May 2013 – Accepted: 18 June 2013 – Published: 6 August 2013

Abstract. The diurnal variation of HOCl and the related species ClO, HO_2 and HCl measured by satellites has been compared with the results of a one-dimensional photochemical model. The study compares the data from various limb-viewing instruments with model simulations from the middle stratosphere to the lower mesosphere. Data from three sub-millimetre instruments and two infrared spectrometers are used, namely from the Sub-Millimetre Radiometer (SMR) on board Odin, the Microwave Limb Sounder (MLS) on board Aura, the Superconducting Submillimeter-wave Limb-Emission Sounder (SMILES) on the International Space Station, the Michelson Interferometer for Passive Atmospheric Sounding (MIPAS) on board ENVISAT, and the Atmospheric Chemistry Experiment Fourier Transform Spectrometer (ACE-FTS) on board SCISAT. Inter-comparison of the measurements from instruments on sun-synchronous satellites (SMR, MLS, MIPAS) and measurements from solar occultation instruments (ACE-FTS) is challenging since the measurements correspond to different solar zenith angles (or local times). However, using a model which covers all solar zenith angles and data from the SMILES instrument which measured at all local times over a period of several months provides the possibility to verify the model and to indirectly compare the diurnally variable species. The satellite data were averaged for latitudes of 20° S to 20° N for the SMILES observation period from November 2009 to April 2010 and were compared at three altitudes: 35, 45 and 55 km. Besides presenting the SMILES data, the study also shows a first comparison of the latest MLS data (version 3.3) of HOCl, ClO, and HO_2 with other satellite observations, as well as a first evaluation of HO_2 observations made by Odin/SMR. The *MISU-1D* model has been carefully initialised and run for conditions and locations of the observations. The diurnal cycle features for the species investigated here are generally well reproduced by the model. The satellite observations and the model agree well in terms of absolute mixing ratios. The differences between the day and night values of the model are in good agreement with the observations although the amplitude of the HO_2 diurnal variation is 10–20 % lower in the model than in the observations. In particular, the data offered the opportunity to study the reaction $ClO+HO_2 \rightarrow HOCl+O_2$ in the lower mesosphere at 55 km. At this altitude the HOCl

night-time variation depends only on this reaction. The result of this analysis points towards a value of the rate constant within the range of the JPL 2006 recommendation and the upper uncertainty limit of the JPL 2011 recommendation at 55 km.

1 Introduction

Hypochlorous acid, HOCl, is considered to be a reservoir for active chlorine, ClO_x, and odd hydrogen, HO_x, in the stratosphere and the lower mesosphere (von Clarmann et al., 2012). It is produced primarily by the reaction of ClO and HO_2 (peroxy radical) and is destroyed mainly by photodissociation at wavelengths shorter than 420 nm which returns OH and Cl radicals (Hickson et al., 2007).

$$ClO + HO_2 \rightarrow HOCl + O_2 \quad \text{(R1)}$$

$$HOCl + h\nu \rightarrow Cl + OH \quad \text{(R2)}$$

There are other pathways for the destruction of HOCl, through reactions with atomic chlorine, OH radicals and atomic oxygen, however these reactions are minor mechanisms (Chance et al., 1989). Furthermore, in the polar vortices HOCl is generated by heterogeneous chemistry and contributes to polar ozone loss events (Hanson and Ravishankara, 1992; Abbatt and Molina, 1992). Since Reaction (R1) is the most important gas phase reaction leading to the formation of stratospheric and mesospheric HOCl, model calculations are sensitive to the rate constant, k_1, of this reaction. There have been a number of studies attempting to determine k_1 at room temperature (Reimann and Kaufman, 1978; Leck et al., 1980; Burrows and Cox, 1981). Additionally, some studies have reported a temperature dependence of the rate coefficient (Stimpfle et al., 1979; Nickolaisen et al., 2000; Knight et al., 2000). However, there is a large discrepancy in the laboratory measurements of k_1, which can lead to disagreement between modelled and measured HOCl. Kovalenko et al. (2007) reported that the value of k_1 published by Stimpfle et al. (1979) is a factor of two higher than JPL 2006 recommendations (Sander et al., 2006) and is more consistent with their measurements. The conclusion of Kovalenko et al. (2007), based on two balloon-borne instruments (FIRS-2, Far-InfraRed emission Spectrometer and MkIV, mid-infrared solar absorption spectrometer), has been confirmed by von Clarmann et al. (2009). The rate constant, k_1, has later been revised in JPL 2009 (Sander et al., 2009) and JPL 2011 (Sander et al., 2011) (JPL 2009 and JPL 2011 are identical). The Stimpfle et al. (1979) formula for calculation of the rate constant is based on non-Arrhenius behaviour of the rate coefficient with strong negative temperature dependency, while JPL 2006 (Sander et al., 2006) to JPL 2011 (Sander et al., 2011) use a standard Arrhenius expression.

There have been a variety of stratospheric measurements of HOCl. von Clarmann et al. (2009) have summarised HOCl measurements made so far from balloon-, space- and airborne infrared solar absorption observations (Larsen et al., 1985; Toon et al., 1992; Raper et al., 1987), balloon-borne infrared and far infrared limb-viewing emission measurements (Chance et al., 1989; Johnson et al., 1995; von Clarmann et al., 1997) and satellite measurements. Global HOCl observations were first provided by the Michelson Interferometer for Passive Atmosphere Sounding (MIPAS) (von Clarmann et al., 2006) and further by the Microwave Limb Sounder (MLS) on board the Aura satellite (Waters et al., 2006). More recently, the Superconducting Submillimeter-wave Limb-Emission Sounder (SMILES) provided observations of the vertical distribution and diurnal variation of HOCl, ClO and HO_2 in the stratosphere and lower mesosphere (Kikuchi et al., 2010; Kuribayashi et al., 2013). The ClO diurnal and seasonal variation measured by MLS on board the UARS satellite was provided by Ricaud et al. (2000) from the year 1991 to 1997 in the mid-latitude range (40–50° N). Observations were compared with the results from a zero-dimensional photochemical model as well as a three-dimensional chemical transport model. Sato et al. (2012) have recently compared these 7 yr average UARS data with the ClO mid-latitude diurnal variation from SMILES (January to February 2010) in the stratosphere and mesosphere. This was the first observation of the full diurnal variation of ClO in the mesosphere. Interestingly, the ClO abundance is enhanced during the day in the stratosphere and during the night in the mesosphere.

Data from several new limb instruments became available in the last decade with the launch of Odin in 2001, MIPAS in 2002, ACE-FTS in 2003, MLS in 2004, and finally SMILES in 2009. In this paper we compare the results of a one-dimensional (1-D) photochemical model with concentrations of HOCl, ClO, HO_2 and HCl measured by these satellite instruments in the tropical middle stratosphere to lower mesosphere altitude region. We investigate the diurnal variation of the species at low latitudes and at the altitudes of 35, 45 and 55 km during the period of SMILES observations from November 2009 to April 2010. Here, unless otherwise noted, the measured profiles, between 20° S and 20° N, were interpolated onto a fine altitude grid, binned into about 2.5–3° wide bins of solar zenith angle, and averaged over one month. The aim of this paper is to compare the observations of these fairly new instruments with each other and with model simulations in order to assess the consistency of the datasets and to test our understanding of atmospheric chemistry. In particular, HO_2 data from Odin/SMR have not been compared with other observations before and hence this paper presents the first validation of SMR HO_2 data. Comparisons of the most recent versions of Odin and SMILES data with the latest version of MLS retrievals (version 3.3) are presented in this paper. The inter-comparison of satellite sensors is a difficult task for short-lived species, since the instruments measure typically at different solar zenith angles. Sensors on sun-synchronous orbits have different equator crossing times

(Aura/MLS ∼ 1.30 a.m./p.m., Odin/SMR ∼ 6 a.m./p.m., and MIPAS ∼ 10 a.m./p.m.), whilst solar occultation sensors (ACE-FTS) measure at a solar zenith angle of about 90°. The modelling of diurnal cycles of species provides a means of indirectly comparing these observations. We employed therefore a particularly suitable method, based on the diurnal variation calculated by a 1-D model, to perform a comprehensive comparison between the satellite observations at different solar zenith angles. The quality of the model is assessed by comparison with diurnal cycles from the satellites. The diurnal variations of ClO, HCl, HO_2 and HOCl are studied only from the middle stratosphere to the lower mesosphere, where the interference with NO is minimal (Jucks et al., 1998). In particular, at mesospheric altitudes, the diurnal amplitude of HOCl is less dependent on nitrogen and atomic oxygen chemistry. Hence, an important point of this analysis is the evaluation of the rate constant of Reaction (R1) in the mesosphere. This point is also noted by Kuribayashi et al. (2013). The model helps to better understand and confirm the kinetics of the reactions involved.

The satellite measurements used in this study are described in Sect. 2. Section 3 provides details on the model and the simulations of HOCl, ClO, HO_2 and HCl. The results of the satellite and model comparisons as well as a study of HOCl reaction rates are presented in Sect. 4. Conclusions are drawn in Sect. 5.

2 Measurements

The observations are described in two subsections corresponding to the measurement method. Odin/SMR, Aura/MLS and SMILES are sub-millimetre limb sounding measurements, whilst MIPAS and ACE-FTS are thermal emission and solar occultation infrared limb-viewing measurements, respectively.

2.1 Sub-millimetre wave limb-viewing measurements

The Sub-Millimetre Radiometer (SMR) on the Odin satellite, launched in 2001, measures thermal emission at the atmospheric limb using various bands in the 486–581 GHz spectral region (Murtagh et al., 2002; Frisk et al., 2003). The satellite was launched in a sun-synchronous orbit crossing the equator at about 6 a.m. and 6 p.m. Due to the lack of fuel on board the satellite, the SMR equator crossing times changed slowly from 6 a.m. (6 p.m.) to almost 7 a.m. (7 p.m.) during the course of the mission as the orbit altitude decreased from about 620 to 580 km. We use Odin/SMR ClO and HO_2 level-2 data from version 2.1 of the operational processor. ClO was measured using a band centred at 501.8 GHz every second day during the relevant period November 2009 to April 2010. Vertical profiles are typically available between 15 and 65 km with a vertical resolution of 2.5–3 km up to roughly 45 km and degrading considerably above 45–50 km where the vertical sampling interval changes in this particular observation mode. The total systematic error of ClO measured by SMR between 20 and 50 km is estimated to be smaller than 0.02 ppbv (5 %) (Urban et al., 2005). A more detailed description of the ClO dataset and an intercomparison with coincident profile measurements made by Aura/MLS are provided by Urban et al. (2005, 2006) and Santee et al. (2008). HO_2 is measured in a band centred at 576.9 GHz. As the frequency of this radiometer is normally not stable due to a hardware failure (phase-lock) (Dupuy et al., 2004), only data for a short period from October 2003 to October 2004 have so far been analysed and are used in this study. HO_2 measurements were performed on only one observation day per month. Baron et al. (2009) provides a description of the characteristics of the Odin/SMR HO_2 dataset. In contrast to Baron et al. (2009), who used an off-line retrieval approach, we use the operational Odin/SMR single-profile retrieval product providing data between about 30 and 60 km with a vertical resolution varying from 4 to 8 km within this range. The operational HO_2 data have so far not been compared to other measurements.

The Microwave Limb Sounder (MLS) on board the Aura satellite has been operating since 2004. MLS has a sun-synchronous near-polar orbit and measures vertical profiles of various species from the upper-troposphere to the lower mesosphere in the millimetre and sub-millimetre spectral regions (Barret et al., 2006; Froidevaux et al., 2008; Santee et al., 2008; Pickett et al., 2008). We have used the version 3.3 products for HOCl, HCl, HO_2 and ClO. MLS measures the same spectral lines of HCl and ClO as SMILES (around 625 and 649 GHz, respectively). The vertical resolution is 3–6 km for HOCl, 3–5 km for HCl, 3–4 km for ClO and 4–5 km for HO_2. The MLS data with negative error and bad quality have been removed according to the MLS user's guide documentation (Livesey et al., 2011). The MLS scientific team recommends HOCl data to be used only up to 2.2 hPa (∼ 42 km) and ClO data up to 1 hPa (∼ 48 km). We have, however, used the HOCl data at 45 km after removing the bad quality data. The MLS profiles in each solar zenith angle bin are averaged on pressure levels over one month. The averaged profile is interpolated onto a single geopotential altitude grid. The geopotential altitude grid is calculated by averaging the geopotential altitudes measured by MLS during the period and the latitude considered in this analysis. The accuracy for HOCl measured by MLS in the altitude range 2.2 to 10 hPa (∼ 31–42 km) is estimated to be about 30–80 pptv (± 30–100 %). A systematic scaling uncertainty for ClO is given as 5–15 % at 15–1.5 hPa (∼ 28–45 km), and the bias uncertainty is ±0.05 ppbv for the same range. A systematic scaling uncertainty of about 20 % and 6 % is estimated for HO_2 at altitudes of about 31 km and 48 km, respectively (Livesey et al., 2011).

The Superconducting Submillimeter-wave Limb-Emission Sounder (SMILES) instrument was installed on the International Space Station (ISS) and used 4 K cooled

superconductor detector technology to measure stratospheric and mesospheric species including HOCl, ClO, HO_2 and HCl (Kikuchi et al., 2010). The instrument was developed by the Japan Aerospace Exploration Agency (JAXA) and the National Institute of Information and Communications Technology (NICT). SMILES measured the vertical distribution of various stratospheric and mesospheric species from October 2009 until April 2010 mostly in the latitude range of 38° S–65° N (Kikuchi et al., 2010). Because of the 2-month precession of the ISS non-synchronous orbit, SMILES was able to follow the diurnal cycle of the chemical species. During one scan, two spectral bands are measured among the three predefined ones, named A (624.3–625.5 GHz), B (625.1–626.3 GHz) and C (649.1–650.3 GHz) (for more details, see the SMILES Mission Plan, version 2.1, at http://smiles.nict.go.jp/Mission_Plan/). In this paper, we use the version 2.1 data provided by JAXA (Mitsuda et al., 2011; Takahashi et al., 2010, 2011), here named SMILES-O. We also include the results from the processor (version 2.1.5) developed by NICT, named here SMILES-R (Sato et al., 2012; Sagawa et al., 2013). This version is based on the version 2.0.1 (Baron et al., 2011) but includes significant changes. Differences between the processor versions are described by Kasai et al. (2013). Compared to the analyses presented in Baron et al. (2011), systematic errors in the level-2 data are reduced in by taking into account the nonlinearity of the radiometer gain in the spectral radiance calibration (level-1b version 7) and improvements of the spectroscopic database. The HOCl profiles have a typical vertical resolution of 5, 8 and 12 km at 35, 45 and 55 km, respectively. The HO_2 profiles have an altitude resolution of about 4, 5, and 5 km for the same levels. The typical vertical resolution of ClO is about 4, 4 and 6 km (Sato et al., 2012; Sagawa et al., 2013). The altitude resolution of the $H^{37}Cl$ profile is 3, 4 and 6 km and that of $H^{35}Cl$ is 3, 3 and 5 km at 35, 45 and 55 km, respectively (Baron et al., 2011). A recent publication on SMILES ClO data in the stratosphere by Sagawa et al. (2013) reports good agreement with coincident profiles measured by various instruments including Odin/SMR, Aura/MLS and MIPAS. The estimated systematic error for ClO in the altitude range of 45–55 km is about 10–30 pptv (10 %) and 5–8 pptv (5 %) for daytime and night-time, respectively (Sato et al., 2012). The systematic error of the HOCl measurements by SMILES is about 0.005 ppbv at about 50 km and increases to 0.04 ppbv at 35 km (Baron et al., 2011).

2.2 Infrared limb-viewing observations

The Michelson Interferometer for Passive Atmospheric Sounding (MIPAS) was a mid-infrared limb-viewing emission spectrometer installed on the Environmental satellite (ENVISAT). ENVISAT was launched in 2002 into a sun-synchronous polar orbit (800 km) and stopped operation in April 2012. MIPAS took measurements by looking backwards and to the side for tangent altitudes from 6 to 68 km for the observation of stratospheric species. The vertical sampling of MIPAS was 3 km from 6 to 42 km and 8 km from 42 to 68 km. MIPAS acquired about 75–80 scans per orbit and a typical scan consisting of 15 to 17 limb-viewing measurements took about 70 s. ENVISAT crossed the equator with the descending node at 10:00 LT (local time) and the ascending node at 22:00 LT. The HOCl data used here are from the level 2 product processed at the Karlsruhe Institute of Technology. Due to some instrumental problems, MIPAS was operated at reduced spectral resolution from 2005 onwards, and no more HOCl data are available since then. Therefore, the HOCl data from MIPAS are taken from the period November 2003 to April 2004. The main systematic error component is the uncertainty of spectroscopic parameters, which is estimated to be about 5–10 % (Flaud et al., 2003) and maps directly on the HOCl results. Since uncertainties arising from the temperature dependence also contribute to the error, a systematic error of about 10 % can be assumed for HOCl (von Clarmann et al., 2006).

The Atmospheric Chemistry Experiment Fourier Transform Spectrometer (ACE-FTS) was launched on board the Canadian SCISAT satellite in 2003. The SCISAT low altitude (650 km), high inclination (74°) circular orbit allows a coverage of polar to tropical regions. The ACE-FTS instrument has a spectral resolution of 0.02 cm^{-1} from 750–4400 cm^{-1} and a vertical resolution of 3–4 km from the cloud tops to 150 km. The instrument collects infrared solar spectra from 15 sunrise and sunset occultations per day (Bernath et al., 2005; Boone et al., 2005; Mahieu et al., 2008). The HCl data from the level 2 product of version 2.2 from November 2009 to April 2010 in the tropics are used in this study. To filter out the outliers present in this version of ACE-FTS data, the monthly median instead of the mean is used in each solar zenith angle bin.

3 Model and simulations

MISU-1D is a 1-D photochemical box model incorporating detailed radiative transfer calculations in the UV and visible region and state of the art stratospheric and mesospheric chemistry (Jonsson, 2006). Multiple scattering and albedo effects are treated according to Meier et al. (1982). The sphericity of the Earth is taken into account which allows for non-zero transmitted flux at solar zenith angles greater than 90 degrees. The Earth-Sun distance is corrected for seasonal variations according to Madronich (1993). The variability in the solar flux over the 11 yr solar cycle is not considered in this study. The model includes a total of 120 reactions, constituting the most important gas-phase reactions in the stratosphere and mesosphere. The kinetic parameters for the calculation of rate constants and photolysis rates are mostly specified according to JPL 2006 recommendations, except for the reactions involving HOCl, HO_2 and HCl, which have been

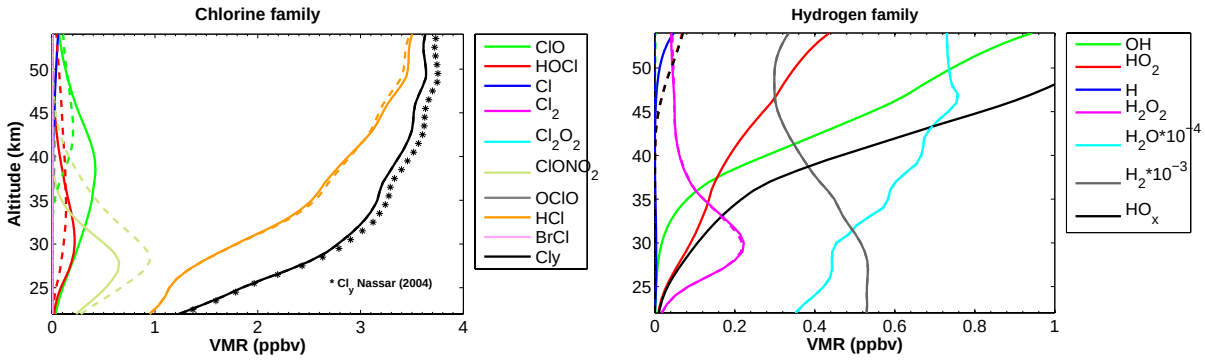

Fig. 1. Chlorine species profiles (on the left) and hydrogen species profiles (on the right) simulated for conditions of 1 November in the tropics. The total inorganic chlorine in the model is constrained according to measurements by ACE-FTS from 30° S to 30° N and altitudes 10 to 60 km (Nassar et al., 2006), but corrected for the temporal decrease of HCl from year 2004 to 2009. Water is initialised according to water profiles measured by MLS on 1 November 2009. Temperature and pressure profiles are taken from ECMWF analyses for the same day. Profiles of the model species at noon are shown as solid lines and profiles at midnight as dashed lines.

updated to JPL 2011 (Sander et al., 2011), and the rate of Reaction (R1), which is specified according to Stimpfle et al. (1979). The input solar flux for the calculation of photolysis rates is adopted from the WMO (1986) reference spectrum. Ozone absorption cross sections and the oxygen absorption cross sections in the Schumann-Runge bands are in accordance with WMO (1986) recommendations and the Koppers and Murtagh (1996) algorithm, respectively. The Herzberg continuum is taken from Nicolet and Kennes (1986).

Temperature and pressure profiles for the simulated period November 2009 to April 2010 are taken from European Centre for Medium-Range Weather Forecasts (ECMWF) analyses. The concentration of gases in the model is initialised with output from the Canadian Middle Atmosphere Model (CMAM). Short-lived species (e.g. radicals) are initialised with zero concentrations and are generated by the chemical reactions in the model. The initialisation in the model is crucial to get a reliable result which matches the observations. For this purpose, total inorganic chlorine, Cl_y, is constrained according to ACE-FTS and SMR observations in 2004 from 30° N to 30° S and altitudes 10 to 60 km (Nassar et al., 2006). The temporal decrease of Cl_y from 2004 to 2009 of ~ 0.6 % per year is taken into account (WMO, 2010; Jones et al., 2011a). Water vapour is initialised according to MLS observations (version 3.3) from November 2009 to April 2010 and between 20° N to 20° S. A methane profile is taken from the built-in CMAM climatology which was found to agree well with the observations by ACE-FTS, MIPAS and HALOE (HALogen Occultation Experiment) (Wrotny et al., 2010). Total inorganic nitrogen, NO_y, is constrained using ACE-FTS observations (5 yr climatology) from 20° N to 20° S (Jones et al., 2011b). Figure 1 shows vertical profiles of chlorine and hydrogen species in the model at noon and midnight for solar conditions of 1 November at the equator. HCl is clearly the largest contributor to Cl_y, with secondary contributions from ClO, HOCl and $ClONO_2$ in the lower and middle stratosphere and from ClO and HOCl in the upper stratosphere and lower mesosphere. H_2O and H_2 are the main contributors to the hydrogen family in all altitudes. The secondary contributors are OH and HO_2 from 35 to 55 km. Between 25 and 35 km, H_2O_2 dominates HO_x ([OH]+[HO_2]+[H]). The model is initialised for a specified time and location (latitude-longitude point) after which simulations can be performed either with a fixed or variable sun position. Here we consider a variable sun position to generate day-night cycles. The model then runs for at least 40 days until the diurnal cycles of species concentrations change only insignificantly between subsequent days. During the simulations, photolysis rates are extracted from a look-up table which is recalculated every 24 h using ozone concentrations calculated by the model. The reaction rate constants are calculated separately for each reaction depending on the temperature and are saved in a matrix for further use in differential equations. The chemical module solves a system of stiff ordinary differential equations with a variable order method according to Shampine and Reichelt (1997). This algorithm solves the time evolution of each species present in the reaction scheme (Jonsson, 2006).

The model has been applied for conditions of the times and locations of the SMILES measurements. This means that the length of the day and sunrise/sunset changes in the model correspond to the latitudes and seasonal effects in the measurements. We calculate the temporal development of HOCl, ClO, HO_2 and HCl at 35, 45 and 55 km for the latitudes 20° S, 0° and 20° N and for the first day of each month in the time period from November to April. Figure 2 shows the diurnal variation of the chlorine and hydrogen species for solar conditions of 1 November at the equator. The diurnal variations are further discussed in Sect. 4.2.

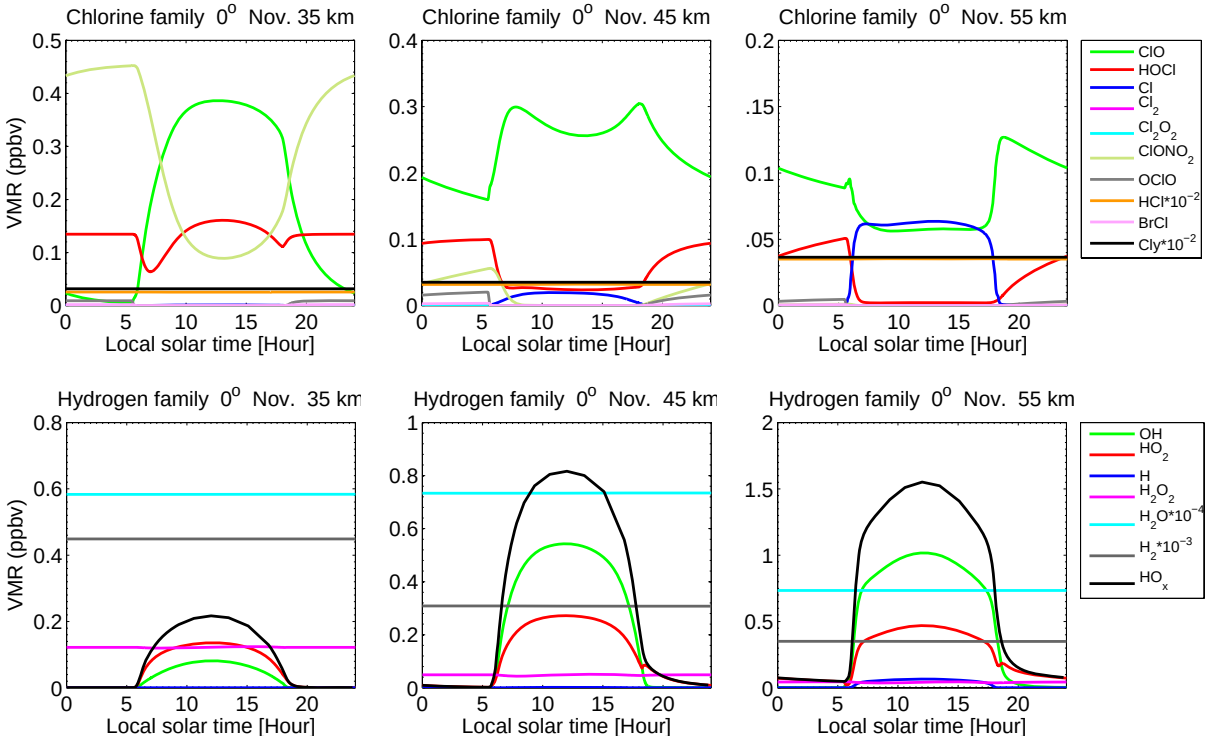

Fig. 2. Modelled diurnal variation of chlorine species (top row) and hydrogen species (bottom row) in the tropics (latitude 0°) calculated for 1 November and altitudes of 35, 45 and 55 km (left, middle and right). The diurnal variation of species are presented as volume mixing ratio versus local solar time. HCl and Cl_y (in the first row) and H_2O and H_2 (in the second row) have been scaled down for better visualisation of minor species (see legend). HO_x is the sum of OH, HO_2 and H.

4 Results and discussion

4.1 Observations

Figures 3 and 4 compare the diurnal variation of HOCl and the related species, ClO, HO_2 and HCl in observations from SMILES, MLS, SMR, MIPAS and ACE-FTS with the *MISU-1D* model simulations. The differences between different data sets and SMILES have been quantified in Table 1. Throughout this study the observation results are, unless otherwise noted, averaged between 20° S to 20° N and over the full-life time period of SMILES from November 2009 to April 2010. For ACE-FTS HCl, the median is used instead of the mean in each solar zenith angle bin. The error bars represent the standard error of the mean observation for each individual data point. SMILES is represented by two different datasets, namely SMILES-O and SMILES-R. Whenever the two SMILES products differ in measured values, the differences between the SMILES products and the other datasets are shown as a range in Table 1. SMR, MIPAS and MLS provide data in a limited range of solar zenith angles, corresponding to the ascending and descending nodes at the equator of the respective satellite. ACE-FTS observations are limited to sunrise and sunset occultations. HO_2 data from MLS are corrected for bias by taking into account day-night differences and assuming negligible HO_2 during night-time according to the MLS user's guide documentation (Livesey et al., 2011). HO_2 data from SMR are averaged over the period October 2003 to October 2004 and HOCl data from MIPAS are averaged from November 2003 to April 2004, as these data are not available for the period November 2009 to April 2010. Consequently, some deviations in HOCl from MIPAS and HO_2 from SMR may be attributed to the different observation periods. The variability of each group of measurements is shown as a vertical error bar representing the respective 1-σ standard deviation. Next, in order to remove the offset between the different datasets and to investigate the amplitude of the diurnal variations, the mean of the night-time or morning volume mixing ratios at the respective levels is subtracted from the observations at other solar zenith angles. For SMILES and the model, the night-time volume mixing ratios for the solar zenith angle range measured by MLS (solar zenith angles between $-130°$ to $-160°$) are subtracted from daytime volume mixing ratios. The data are then shifted to match the SMILES-R data in the same solar zenith angle range (night). The results are shown in Figs. 5 and 6. This method decreases the discrepancies between the different satellite measurements and the simulations arising from biases in the datasets.

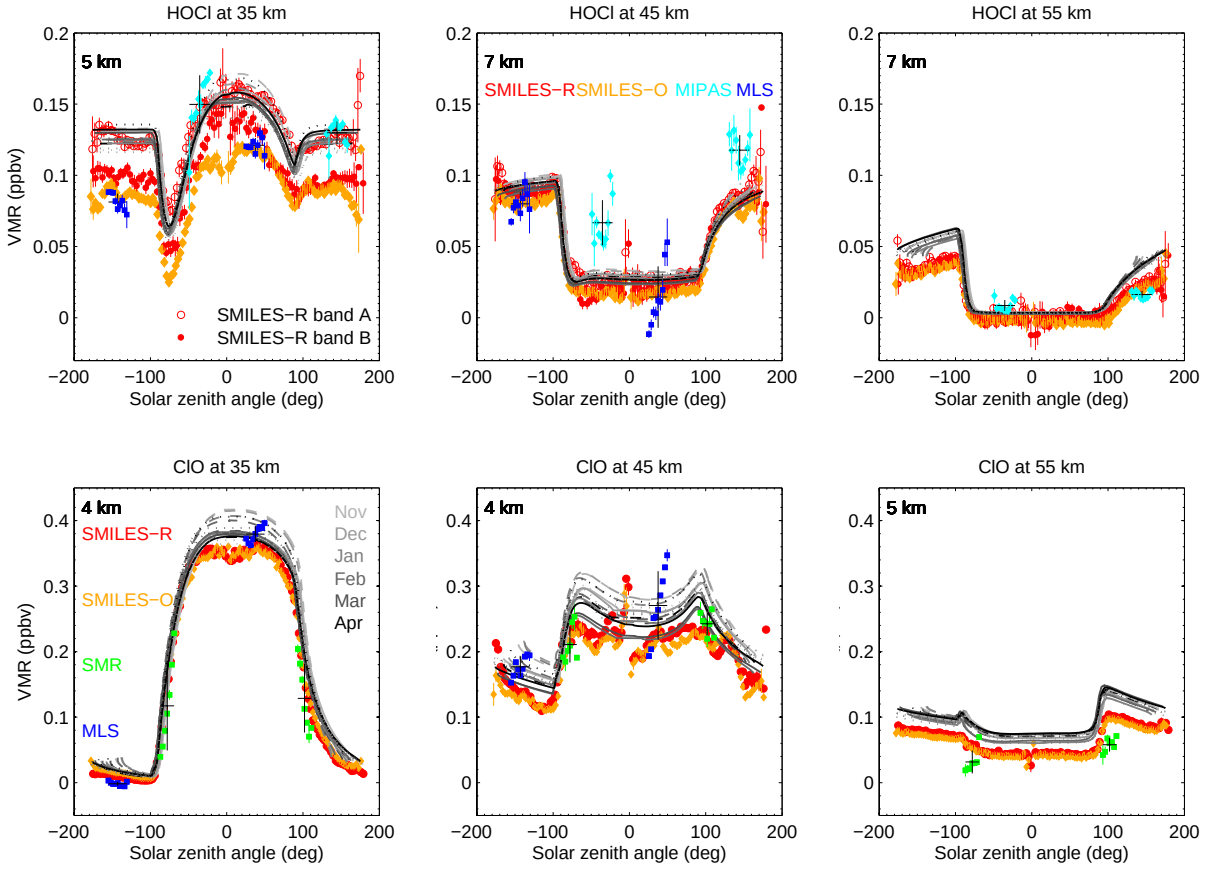

Fig. 3. Modelled diurnal variation of HOCl and ClO at the altitudes 35, 45 and 55 km (left, middle, right) in the tropics between 20° S and 20° N compared to observations made by SMILES, Aura/MLS, Odin/SMR and ENVISAT/MIPAS during the period November 2009 to April 2010. SMILES data are presented by two products; the research product (here called SMILES-R) and the official product (here named SMILES-O). Top row: HOCl; Bottom row: ClO. The standard error of the mean is shown in the same colour as the measurements. If not visible, errors are smaller than the symbol size. Model simulations are given for different months (light grey shaded lines: November; dark grey: April). Solid grey lines are for the equator, dotted lines are for 20° S and dashed lines are for 20° N. Satellite data have been averaged in bins of 2.5–3° in terms of solar zenith angle. HOCl data from MIPAS are averaged from November 2003 to April 2004. The model was run with a vertical resolution of 1 km and the model results have been vertically smoothed using a Gaussian function. The full-width-at-half-maximum (in km) is stated in the left upper corner of each plot. MLS, SMR and MIPAS values have been averaged at their ascending/descending nodes. The variability of these measurements in the form of 1-σ standard deviation is shown as vertical error bars in black. The horizontal error bars show the range of solar zenith angles of the respective measurements.

For HOCl (first row of Fig. 3), the MLS and MIPAS measurements follow the diurnal cycle measured by SMILES and calculated by the model quite well, i.e. the difference between ascending and descending nodes of the MLS and MIPAS data corresponds well with the results from SMILES observations at the corresponding solar zenith angles. However, there are some differences. The SMILES HOCl observations are measured in bands A and B. The SMILES JAXA product (SMILES-O) is retrieved from band A, while the NICT product (SMILES-R) is retrieved from both bands A and B (same spectral line but different radiometer settings). The designed frequency region of band B is 625.12–626.32 GHz. In fact, the measured frequency region is wider than the nominal one and HOCl was observed at the edge of band B. Here, we compare the two bands for SMILES-R, although HOCl in band B is at the band edge and its quality is expected to be worse than in band A. At 35 km, there are some differences between band A and B from SMILES-R, but the differences are within the uncertainty arising from the systematic error of SMILES-R (0.04 ppbv). MIPAS measures similar HOCl values as SMILES-R band A (the maximum of the SMILES range), whilst MLS measures HOCl values closer to SMILES-R band B and SMILES-O (the minimum of the SMILES range). The two SMILES-R bands and SMILES-O agree well at 35 and 45 km. In the upper stratosphere at 45 km, MLS and all SMILES datasets agree well in terms of the absolute values, with the mean of MLS being in the range of the SMILES observations. MIPAS HOCl

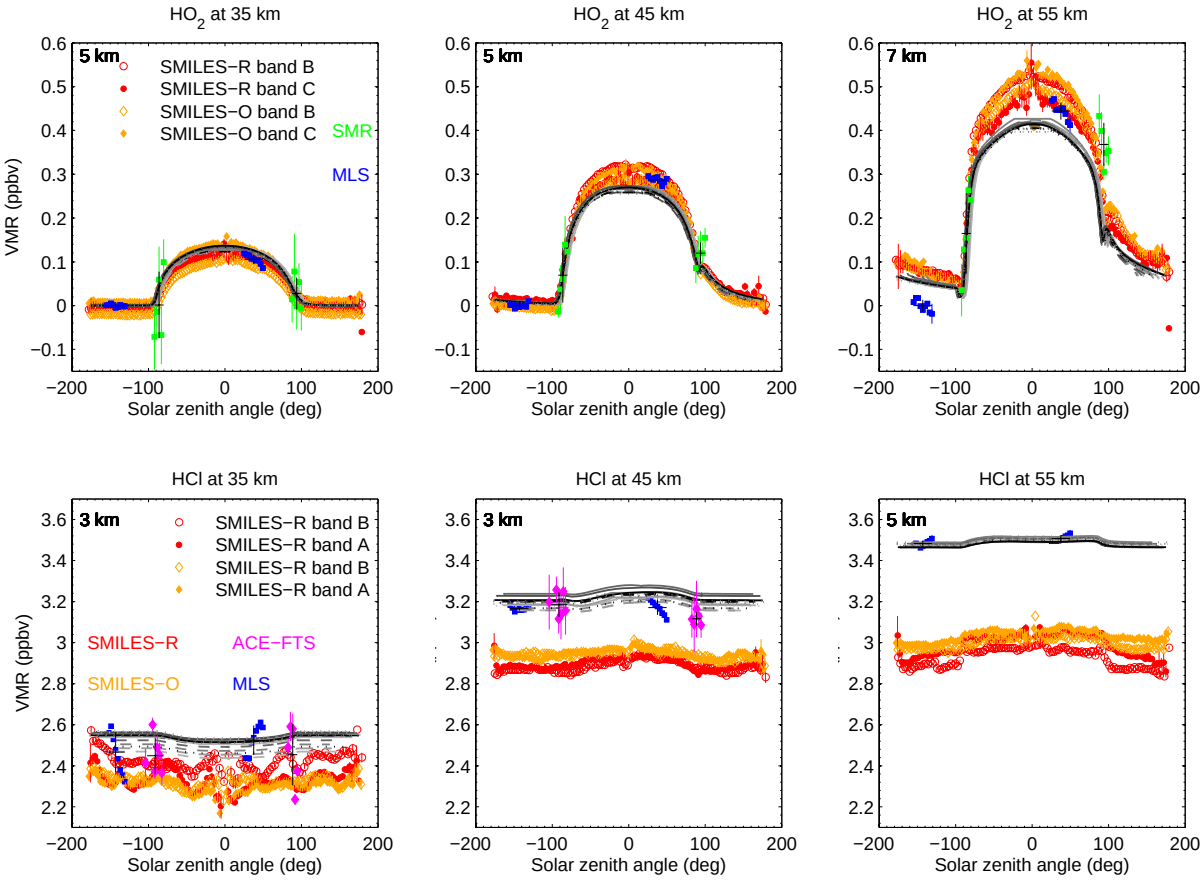

Fig. 4. Same as Fig. 3, but showing modelled and observed diurnal variation of HO_2 and HCl made by SMILES, Aura/MLS, Odin/SMR and SCISAT/ACE-FTS at the altitudes 35, 45 and 55 km (left, middle, right) during the period November 2009 to April 2010. Top row: HO_2; bottom row: HCl. HO_2 from SMR corresponds to the period October 2003 to October 2004. MLS, SMR and ACE-FTS values have been averaged at their ascending/descending or sunrise/sunset nodes.

measurements are about 0.04 ppbv larger than the other observations at this altitude. The difference is larger than the combined systematic error of SMILES-R and MIPAS which is smaller than ∼ 0.017 ppbv. The difference between the MIPAS dataset and the other observations at these three altitudes should at least in part be due to the earlier time period of the MIPAS observations (using data from 2003/2004 as opposed to 2009/2010), as total inorganic chlorine (Cl_y) has been decreasing from about year 2000 onwards at this altitude (WMO, 2010). A further explanation is that the vertical resolution of MIPAS HOCl profiles becomes worse above 40–45 km, and smearing out a concave branch of the profile can bias the values high. Additionally, due to the larger solar activity in 2003/2004 compared to 2009/2010 (close to solar minimum), more OH production is expected (Wang et al., 2013). The enhanced OH leads to higher HO_2 and may have consequently increased the formation of HOCl by Reaction (R1). The daytime MLS observations at 45 km are more variable than those of MIPAS and SMILES showing a variability of 0.02 ppbv (1-σ standard deviation) at solar zenith angles ranging from 25° to 49°. In the lower mesosphere at 55 km, the MIPAS and SMILES HOCl mixing ratios show good agreement and the mean of the differences does not exceed 0.008 ppbv. The MIPAS sensitivity, however, is largely reduced at higher altitudes.

In the first row of Fig. 5, the satellite observations of HOCl have been compared after offset correction to match the SMILES data. The amplitudes of the HOCl diurnal cycle deduced from MLS, SMILES, and MIPAS agree reasonably well at 35 and 45 km (the mean differences do not exceed 0.01 and 0.02 ppbv, respectively), however at 55 km the MIPAS diurnal cycle amplitude is about 0.02 ppbv smaller than that of SMILES.

ClO measurements by SMILES, MLS and SMR are presented in the second row of Fig. 3. At 35 km, the absolute values of ClO in volume mixing ratio agree quite well (differences do not exceed 0.03 ppbv), however there are some minor differences (Table 1). At 45 km, the SMR and SMILES (SMILES-R and SMILES-O) data agree reasonably well within about 0.02 ppbv. At the same altitude,

Table 1. Differences between the observations of HOCl, ClO, HO_2 and HCl from MLS, SMR, MIPAS and ACE-FTS with the data from SMILES (SMILES-O version 2.1 and SMILES-R version 2.1.5) at three altitudes (35, 45 and 55 km). Differences (satellite minus SMILES) are given in ppbv. Ranges are indicated corresponding to the differences between the SMILES products.

HOCl				
	MLS		MIPAS	
SMILES	night	day	night	day
35 km	−0.005 to −0.05	+0.005 to −0.04	+0.01 to +0.04	0 to +0.05
45 km	−0.01	−0.01	+0.03 to +0.04	+0.04 to +0.05
55 km	–	–	−0.01	+0.01
ClO				
	MLS		SMR	
SMILES	night	day	a.m.	p.m.
35 km	−0.01	+0.02	∼ +0.03	∼ +0.03
45 km	+0.04	+0.05	−0.02	+0.02
55 km	–	–	−0.03	−0.04
HO_2				
	MLS		SMR	
SMILES	night	day	a.m.	p.m.
35 km	$< \pm 0.02$	$< \pm 0.02$	0 to −0.02	0 to +0.02
45 km	$< \pm 0.02$	$< \pm 0.02$	∼ 0	+0.03
55 km	−0.08	0 to −0.07	∼ 0	∼ +0.12
HCl				
	MLS		ACE-FTS	
SMILES	night	day	a.m.	p.m.
35 km	+0.05 to +0.15	+0.15 to +0.24	+0.02 to +0.13	+0.04 to +0.16
45 km	+0.24 to +0.32	+0.21 to +0.26	+0.26 to +0.34	+0.18 to +0.26
55 km	+0.53 to +0.61	+0.47 to +0.56	–	–

MLS daytime measurements vary significantly compared with SMILES measurements within the range of solar zenith angles from 20 to 50°. The daytime ClO from MLS varies by about 0.05 ppbv (1-σ standard deviation) from its mean value (0.27 ppbv). At this altitude, the mean of MLS night-time and daytime observations are higher than corresponding SMILES measurements by almost 0.04 and 0.05 ppbv, respectively (Table 1). Both SMILES ClO datasets at 55 km show more ClO than sunrise and sunset observations by SMR and the differences are about 0.04 ppbv. Compared to the systematic errors of SMR (0.02 ppbv) and SMILES-R (night: 5–8 pptv, day: 10–30 pptv), the difference between these two datasets is only significant during night-time. Note that the statistical errors of SMILES are considerably lower than the systematic errors (Sato et al., 2012). In the second row of Fig. 5, the offset corrected observations are shown. The amplitudes of the observed diurnal variations agree reasonably at all altitudes (the absolute mean of differences does not exceed 0.05 ppbv), however there are some dissimilarities. At 35 km, the MLS amplitude is about 0.05 ppbv larger than the SMILES amplitude. The amplitude of SMR data at 45 km is about 0.03 ppbv larger than that of SMILES and about 0.03 ppbv smaller at 55 km.

The first row of Fig. 4 shows the HO_2 observed by MLS, SMILES and SMR at three altitudes. HO_2 measured by SMILES, SMR and MLS compares relatively well at all the altitudes of interest, particularly at 35 and 45 km, where the mean of the differences does not exceed 0.02 ppbv. The differences between the SMILES datasets and the other observations are shown in Table 1. At 35 km, in spite of the variability of the SMR HO_2 measurements around the solar zenith angle of −90°, the mean of SMR agrees quite well with both SMILES bands (the mean of the differences is about 0.02 ppbv). Although SMILES-R band B data maybe slightly less precise than band C, we have chosen both bands for comparison in order to evaluate the measurements against each other. At this level, the results from SMILES-R and SMILES-O band B have both negative values at night-time.

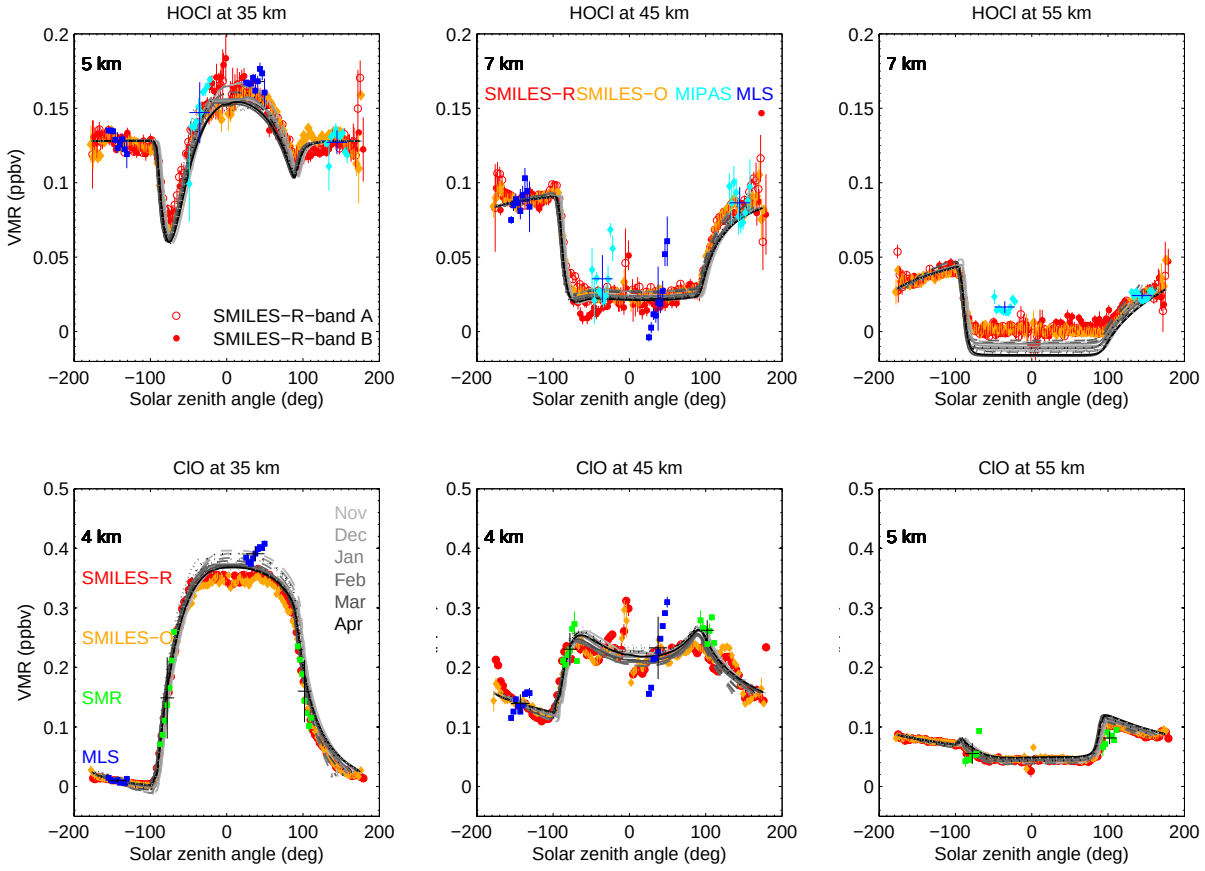

Fig. 5. Same as Fig. 3, but offset shifted for high solar zenith angles at night-time or sunrise in order to compare the amplitudes of the SMILES, MLS, SMR and MIPAS diurnal cycles with the model. The average night-time or sunrise satellite measurements in the overlapping solar zenith angles and the model were subtracted from the values at other solar zenith angles and a correction term respective to SMILES-R for the same solar zenith angle range has been added.

As mentioned in the first paragraph of this section, MLS HO_2 measurements have been corrected for instrumental bias by taking into account the night-day differences. Due to the sun's higher activity, when SMR data were collected (year 2003/2004) compared with the solar minimum activity in 2009/2010 when the other observations were made, SMR observes consistently the highest mixing ratios. Note also that SMR is not zero corrected for night-time HO_2 measurements as MLS, thus a bias cannot be completely excluded. The source of the HO_x family, in fact, is the photo-dissociation of water vapour generated by solar irradiance.

At 45 km, the results from MLS measurement of HO_2 (after bias correction) agree well with the results from the SMILES range of measurements (0.27–0.32 ppbv). HO_2 measured by SMR compares reasonably well with SMILES observations of both bands around sunrise, however the mean of the differences is about 0.03 ppbv around the solar zenith angle of 90° (sunset). In the lower mesosphere at 55 km, SMILES-R and SMILES-O data cover the range of about 0.46–0.55 ppbv at the HO_2 maximum around noon. In the lower mesosphere at 55 km, the mean of night-time and daytime MLS HO_2 (about zero and 0.45 ppbv, respectively) are about 0.08 and 0–0.07 ppbv lower than that of the corresponding SMILES range of observations, respectively. The mean of sunrise SMR observations (about 0.16 ppbv) compares well with the SMILES range of observations, however, the SMR sunset observations (mean of about 0.37 ppbv) are about 0.12 ppbv larger at 55 km. In the first row of Fig. 6, the HO_2 amplitude (the difference of day and night) of the measurements agree well at 35 and 45 km. The amplitude of HO_2 observations by SMR and MLS at 55 km are about 0.15 and 0.05 ppbv larger than that of SMILES, respectively.

In the bottom row of Fig. 4, we show the HCl observations made by MLS, SMILES and ACE-FTS at 35, 45 and 55 km. There are some discrepancies between the different satellite observations of HCl in terms of the absolute values at all the altitudes of interest. As can be inferred from Fig. 4, SMILES agrees with the mean of MLS and ACE-FTS observations within the range of 0.02–0.24 ppbv at 35 km, but it measures the lowest HCl among the observations at 45 and

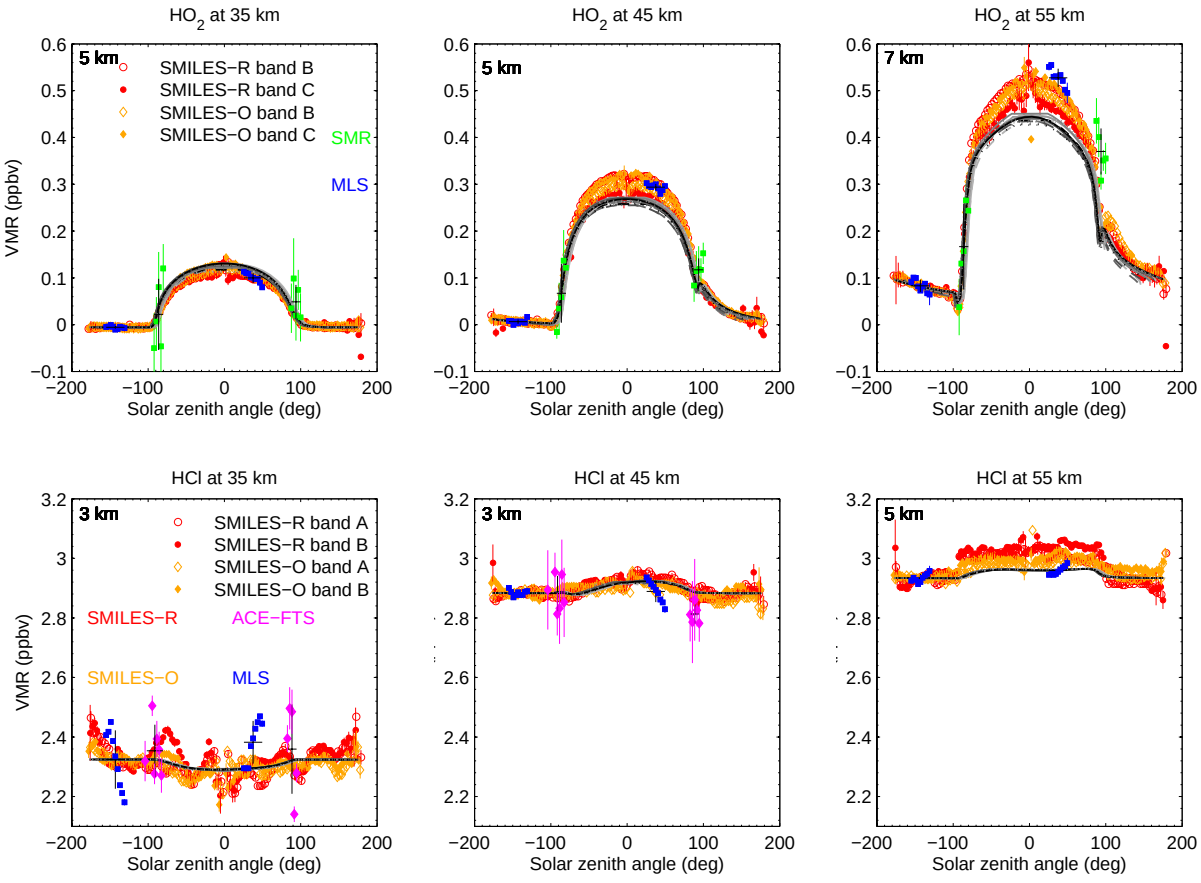

Fig. 6. Same as Fig. 4 but offset shifted for high solar zenith angles at night-time or sunrise in order to compare the amplitudes of the SMILES, MLS, SMR and ACE-FTS diurnal cycles with the model. The average night-time or sunrise satellite measurements in the overlapping solar zenith angles and the model were subtracted from the values at other solar zenith angles and a correction term respective to SMILES-R for the same solar zenith angle range has been added.

55 km. The differences are given in Table 1. The MLS and ACE-FTS data agree well at 45 km and the differences do not exceed 0.05 ppbv. The offset corrected measurements respective to SMILES, shown in the last row of Fig. 6, indicate that all observations show a very small HCl diurnal cycle. There are small differences between the diurnal cycle amplitude measured by SMILES, MLS and ACE-FTS. ACE-FTS and MLS data have slightly larger diurnal cycle amplitudes than the SMILES data at 35 and 45 km, however the differences do not exceed 0.1 ppbv. The number of individual ACE-FTS measurements in the tropics is small (4 to 27 measurements per solar zenith angle bin) compared to the other instruments. This causes larger uncertainties in the averaged data due to the increased statistical error.

In summary, the satellite observations of the HOCl, ClO, HO_2 and HCl diurnal variation generally agree well both in terms of absolute value and shape, with a few exceptions pointed out above.

4.2 Model comparison

Figures 3 and 4 show the model calculation of HOCl, ClO, HO_2 and HCl in grey shades. The observations shown in the figure have already been discussed in the previous section. The model simulations have been carried out for conditions during the SMILES measurement period from November 2009 to April 2010 and three latitudes (20° S, 0° and 20° N) with one simulation per month and latitude, for a total of 18 runs. To account for the different vertical resolution of model and instruments, the model results have been smoothed using a Gaussian function. The assumed full-width-at-half-maximum (FWHM) is stated in the left upper corner of each plot in Figs. 3 to 6. It is impractical to use the individual averaging kernels of each instrument to degrade the vertical resolution of the model results because we compare the simulated values to several sets of observations simultaneously. However, the vertical resolutions of the instruments used in this study are very close for the different species and altitudes shown here. For this purpose, we used the average vertical

Table 2. Differences between the simulations of HOCl, ClO, HO_2 and HCl by the MISU-1D model and the satellite observations at three altitudes (35, 45 and 55 km). Differences (satellite minus model) are given in ppbv. For SMILES, ranges are indicated for different bands, if the species is measured in more than one band indicating the differences between the bands.

HOCl								
	MLS		MIPAS		SMILES-R		SMILES-O	
Model	night	day	night	day	night	day	night	day
35 km	−0.045	−0.035	+0.01	+0.005	−0.01 to −0.03	−0.01 to −0.03	−0.04	−0.04
45 km	−0.01	−0.015	+0.03	+0.04	0 to −0.005	0 to −0.005	−0.01	−0.12
55 km	–	–	−0.005	+0.015	−0.02	−0.025	−0.025	−0.01
ClO								
	MLS		SMR		SMILES-R		SMILES-O	
Model	night	day	a.m.	p.m.	night	day	night	day
35 km	−0.025	−0.02	−0.04	−0.06	−0.02	−0.03	−0.015	−0.03
45 km	−0.01	+0.02	−0.05	−0.027	−0.02	−0.05	−0.02	−0.05
55 km	–	–	−0.055	−0.08	−0.03	−0.03	−0.03	−0.03
HO_2								
	MLS		SMR		SMILES-R		SMILES-O	
Model	night	day	a.m.	p.m.	night	day	night	day
35 km	−0.001	0 to −0.13	−0.03	∼ 0	0 to −0.007	+0.015	0 to +0.01	+0.04
45 km	−0.01	+0.02	∼ 0	+0.025	−0.01to +0.01	+0.01 to +0.06	+0.01	+0.01 to +0.05
55 km	−0.07	+0.02	∼ 0	+0.2	+0.04	+0.04 to +0.1	+0.04	+0.06 to +0.12
HCl								
	MLS		ACE-FTS		SMILES-R		SMILES-O	
Model	night	day	a.m.	p.m.	night	day	night	day
35 km	−0.07	+0.02	−0.06	−0.05	∼ −0.08	∼ −0.08	∼ −0.15	∼ −0.2
45 km	−0.07	−0.05	−0.02	−0.07	∼ −0.35	∼ −0.3	∼ −0.3	∼ −0.25
55 km	+0.01	+0.01	–	–	∼ −0.5	∼ −0.45	∼ −0.45	∼ −0.5

resolution of all instruments for smoothing. We have tested that the impact of using just one common span (FWHM of the Gaussian) for each species is not significant. Model calculations have been shifted in Figs. 5 and 6 to match SMILES observations at night-time along with the other satellite data to investigate the reaction kinetics and the magnitude of the diurnal variation of the species in the model. The diurnal cycle amplitude depends on the initialisation (e.g. Cl_y and H_2O) of the model, while the shape of the diurnal variation depends on reaction rate coefficients and photolysis parameters.

The diurnal variation of HOCl (first row of Fig. 2) exhibits very different patterns depending on the altitude. The peak of HOCl appears around noontime at 35 km and production dominates the loss by photolysis about 3 h after sunrise, in contrast to higher altitudes where the peak occurs at night-time. At 35 km, HOCl formation by Reaction (R1) follows the HO_2 and ClO variations. Photolysis becomes more important at higher altitudes, resulting in a decrease of daytime HOCl. Moreover, due to the larger mixing ratio of HO_2 at higher altitudes, HOCl constantly forms at these altitudes but is photolysed easily. At 45 and 55 km, HOCl drops rapidly at sunrise, has more stabilised minimum concentrations during the course of the day and rises slowly after sunset. At the altitude of 45 km, HOCl is mostly governed by the ClO diurnal cycle. That can be confirmed by the anti-correlation of ClO and HOCl at this altitude. In the mesosphere (altitudes above 55 km), HOCl becomes a nocturnal sink for ClO after sunset due to the reaction of HO_2 and ClO.

As can be inferred from the first row of Fig. 3, the model reproduces a very similar shape of the diurnal variation of HOCl as the measurements at the three altitude levels. Table 2 summarises the differences between the simulations and the satellite datasets. At 35 km, the model simulations match night observations by MIPAS and the SMILES-R range of observations and the differences are less than about 0.03 ppbv. The MLS observations are about 0.05 ppbv lower than the simulations, however this difference does not exceed the range of systematic uncertainty of MLS (30–80 pptv) at this altitude. At 45 km, the model HOCl calculations match very well with the SMILES range of observations and the mean of MLS at day and night, with differences not exceeding 0.015 ppbv. The difference between

the MIPAS and the model at 45 km is larger than the MIPAS systematic error ($\sim 10\,\%$). The model and the daytime observations agree quantitatively well at 55 km, where the differences fall in the range of the SMILES systematic uncertainty (0.005 ppbv). The night-time simulations are however higher than SMILES even considering the corresponding systematic measurement uncertainty at this level (0.005 ppbv). The offset shifted model (respective to SMILES-R band B) is depicted in the first row of Fig. 5. The amplitudes of the HOCl diurnal cycle deduced from the model and observations agree reasonably well within the range of 0.005–0.015 ppbv at 35 and 45 km. The model amplitude is about 0.015 ppbv and 0.025 ppbv larger than that of SMILES and MIPAS at 55 km.

At 35 km, ClO rises sharply at sunrise and has a flat, fairly extended peak during daytime followed by a sharp drop after sunset in the middle stratosphere (see the first row of Fig. 2). The maximum peak of ClO in daytime at this altitude is mainly attributed to the photo-dissociation of $ClONO_2$. The dominant sink of nocturnal ClO is the combination of ClO and NO_2 and formation of $ClONO_2$ (Ko and Sze, 1984; Ricaud et al., 2000). At 45 and 55 km, the ClO diurnal variation is not just governed by HOCl and $ClONO_2$ (as $ClONO_2$ becomes less important with altitude), but is also influenced by odd oxygen chemistry ($O_x = O + O_3$). ClO at these altitudes and higher can react with free oxygen atoms and be converted to Cl atoms, leading to a ClO minimum during daytime.

The modelled diurnal variation of ClO at the three altitudes 35, 45 and 55 km is depicted in the bottom row of Fig. 3. The differences between the model calculation of ClO and the observations are given in Table 2. ClO simulations generally reproduce very similar shapes as the observations at the altitudes of interest. The model calculates slightly higher ClO than the SMILES data at all altitudes. The absolute values of simulations agree well with the MLS observations and the differences do not exceed 0.025 ppbv. SMILES ClO is slightly lower than both simulations and MLS during daytime. The mean of the SMR observations is about 0.04 ppbv lower than that of the simulations. At 45 km, the model reproduces a very similar daytime decrease of ClO consistent with the SMILES observations, as the result of the reaction with free oxygen which converts ClO to atomic chlorine. The daytime chlorine increase can be seen in the second plot of the first row in Fig. 2. The SMILES observations of ClO at this altitude are about 0.02–0.05 ppbv lower than the model result and the mean of the MLS observations. Although the MLS daytime observations are fairly variable at 45 km (~ 0.05 ppbv in terms of 1-σ standard deviation), the mean MLS values agree reasonably well with the model. At this altitude, SMR measures after sunset about 0.027 ppbv ($\sim 10\,\%$) lower ClO mixing ratios than the simulations. At 55 km, the daytime and night-time model calculations are about 0.03 ppbv higher than the SMILES range of observations. SMR also measures about 0.05–0.08 ppbv lower ClO than the model at 55 km. The comparison of the model diurnal cycle amplitudes of ClO, presented in the second row of Fig. 5, shows very similar amplitudes as the model and MLS at 35 and 45 km. The model amplitude of the diurnal variation agrees with that of SMR at 35 km, but is about 0.02 ppbv smaller and about 0.05 ppbv larger than that of SMR at 45 and 55 km, respectively. The model amplitude agrees with that of the two SMILES datasets at 55 km and the mean of differences does not exceed 0.01 ppbv, however it is about 0.04 ppbv and 0.02 ppbv larger than that of SMILES at 35 and 45 km, respectively.

The diurnal variation of HO_2 exhibits a very similar pattern from the middle stratosphere to the lower mesosphere. Very low values at night-time and a sharp rise after sunrise which leads to the peak of HO_2 during the day, indicates the photolysis dependency of HO_2 formation (second row in Fig. 2). The rise of daytime HO_2 is mainly attributed to the reactions of H_2O with $O(^1D)$ in the stratosphere and lower mesosphere, where $O(^1D)$ is a product of ozone photolysis. The daytime mixing ratio increases with height, due to the more abundant atomic oxygen ($O(^1D)$) at higher altitudes. In Fig. 2, HO_x is the sum of OH, HO_2 and H. Methane oxidation is the other source of HO_2. Since OH and HO_2 are tightly coupled through fast photochemical reactions, the source and sink of these molecules are the same. The drop after sunset is mainly due to the reaction of OH with NO_2 or HNO_3. The self reaction of OH and HO_2 is the other sink for both, producing water. The very small transient dip in the model HO_2 mixing ratios at dawn and dusk at 55 km can be observed in the SMILES measurements as well. Before sunrise, the small drop of mixing ratio is due to the reaction of HO_2 and atomic oxygen (which is generated by ozone photolysis). After sunset, the small transient decrease of HO_2 is because of the stop of the reaction of HO_2 with atomic oxygen, then HO_2 is produced by ozone and OH at a much lower rate.

HO_2 model simulations generally behave similarly as the observations and reproduce a very similar shape at all altitudes of interest, according to Fig. 4. At 35 km, the model result agrees reasonably well with the observations and the differences are below 0.04 ppbv. The night-time model calculation of HO_2, the night-time observations and the SMR observations agree well at 45 km and the differences do not exceed 0.01 ppbv. The modelled daytime HO_2 is about 0.01–0.12 ppbv lower than the average of the SMILES and MLS data at 45 and 55 km. This difference is larger than the estimated systematic uncertainty of MLS for HO_2 (± 0.017 ppbv), but it resides within the uncertainty range of MLS at 55 km (± 0.07 ppbv). At these altitudes, although the SMR observations around sunrise are very close to the model, the observations after sunset are about 0.025–0.2 ppbv above the model average. The amplitude of the HO_2 diurnal variation has been compared with the amplitude from satellite data in the first row of Fig. 6. There is a good agreement between the observed HO_2 amplitudes and the model at 35 km and the mean of differences does not exceed 0.02 ppbv, but the model amplitude is about 0.04 ppbv ($\sim 13\,\%$) smaller than the observations at 45 km. At 55 km,

the model amplitude is lower than all observations and the differences range from 0.07 to 0.1 ppbv.

HCl is the main chlorine reservoir in the stratosphere and mesosphere (see the plots in the first row of Fig. 2). HCl has only a weak diurnal variation in the middle and upper stratosphere, but increases slightly during the course of the day in the lower mesosphere. This diurnal variation cannot be seen in Fig. 2, but it is slightly better visualised in Figs. 4 and 6. This can be explained by the increased probability of the reaction of atomic chlorine with HO_2 which generates HCl during daytime, owing to the more abundant chlorine atoms and HO_2 radicals at this level. The amplitude of the diurnal variation of SMILES HCl is strongly dependent on the retrieval parameters and therefore the results must be viewed with caution.

Initialising the model with a realistic HCl profile as the main chlorine reservoir is crucial to get the correct amount of HOCl and ClO. Past trend studies have shown a decrease in the HCl concentration in the stratosphere and mesosphere (Froidevaux et al., 2006; WMO, 2010; Jones et al., 2011a). Here, we constrained the model with the total inorganic chlorine estimated from ACE-FTS and SMR observations between 30° S to 30° N and from 10 to 60 km from Nassar et al. (2006) (Fig. 1) and corrected for the decreasing trend of 0.6(±0.1) percent/year according to WMO (2010) based on HALOE and updated MLS observations (Froidevaux et al., 2006) from 2004–2010 (60° S–60° N averages). Similarly, the analysis of HCl time series by Jones et al. (2011a) between 35 and 45 km in the tropics (20° S–20° N) based on ACE-FTS and HALOE data shows a linear trend of -5.8 ± 1.7 percent decade^{-1}. Here, the model HCl level at 35, 45 and 55 km is about 2.5, 3.25 and 3.5 ppbv, respectively. Although reproducing a similar shape, the model agrees better with the MLS and ACE-FTS data but gives higher HCl than the SMILES observations at all altitudes and the differences increase with height (last row of Fig. 4). This is probably a result of the sensitivity to the related retrieval parameters.

The bottom row in Fig. 6 shows the offset shifted model and observations. The SMILES amplitude of the HCl diurnal cycle, despite the differences in absolute values with the model at 45 and 55 km, agrees well with that of the model at these altitudes. The MLS amplitude agrees roughly with that of the model at 55 km, but the variability of the observations at 35 and 45 km is too large for a meaningful comparison. The ACE-FTS amplitude of the diurnal cycle at 45 km is larger than that of the model and the SMILES amplitudes. It should be noted that some differences in the model and the observations could be due to the fact that the seasonal variability (e.g. transport) is not taken into account in the model calculation. Since we average the field observations over several months for a broad latitude bin, temporal and spatial changes within these bins over time and space can lead to variability in the measured data. The model cannot take care of such variabilities and just takes the temporal solar zenith angle variations into account.

To summarise, generally good agreement is found between the model and the observations, except for the amplitude of the diurnal cycle of HO_2 at 45 and 55 km, which is smaller in the model. Another exception is the difference in the absolute value of HCl. The modelled HCl is always larger than SMILES, whilst it is more consistent with MLS and ACE-FTS at all altitudes. Note that correct initialisation of the model is essential to reach such a good general agreement.

4.3 Kinetics study

In this section, the sensitivity of the modelled HOCl to different reaction rates, k_1, for Reaction (R1) is investigated. k_1 is calculated according to Stimpfle et al. (1979), Nickolaisen et al. (2000), Hickson et al. (2007) as well as the JPL 2006 and 2011 recommendations (Sander et al., 2011, 2006). Model results for the upper and lower uncertainty limit of k_1 according to the JPL 2011 recommendations were also calculated. The recommended value for calculation of k_1 in JPL 2011 is based on the studies by Hickson et al. (2007), Nickolaisen et al. (2000), Knight et al. (2000) and Stimpfle et al. (1979) that studied Reaction (R1) as a function of temperature. Note that the HOCl formation rate constants from JPL 2009 (Sander et al., 2009) are identical to JPL 2011 (Sander et al., 2011).

The partitioning of chlorine in the model, presented in Fig. 7, shows that changes of k_1 would lead to changes of both HOCl and HCl at 35 and 45 km. Additionally ClO is affected at 35 km during daytime and at 45 km during night-time. At 55 km changes of k_1 lead only to changes of HOCl and ClO and only during night-time. HCl is not affected. The 55 km level is therefore the best level to study k_1 given that HCl with its small diurnal variation is not very well constrained by the measurements at 35 and 45 km (see Fig. 4 and 6). Note that the effect of varying k_1 is negligible for the modelled HO_2.

The shape of the HOCl diurnal variation might be influenced by HOCl photolysis as well as by the reaction of HOCl + O. We have conducted sensitivity tests for these reactions. Variation of HOCl photolysis by 30 % has no effect on the absolute values of HOCl at 55 km unlike at 35 km where HOCl is converted to HCl. At 35 km, a 30 % change of the HOCl photolysis rate causes a change of 0.015 ppbv in the HOCl values during day and night. However, the amplitude of the diurnal cycle at 35 km remains nearly unchanged. The sensitivity of the diurnal variation of HOCl to uncertainties of the reaction HOCl + O has also been investigated using stated JPL 2011 uncertainties. The effect at 35 and 55 km is negligible but changes of the daytime HOCl (of about 18 %) were observed at 45 km. The amplitude of the diurnal cycle increases using the reaction rate corresponding to the lower uncertainty range limit of the reaction HOCl + O. To conclude, uncertainties of the other reactions have a negligibly small

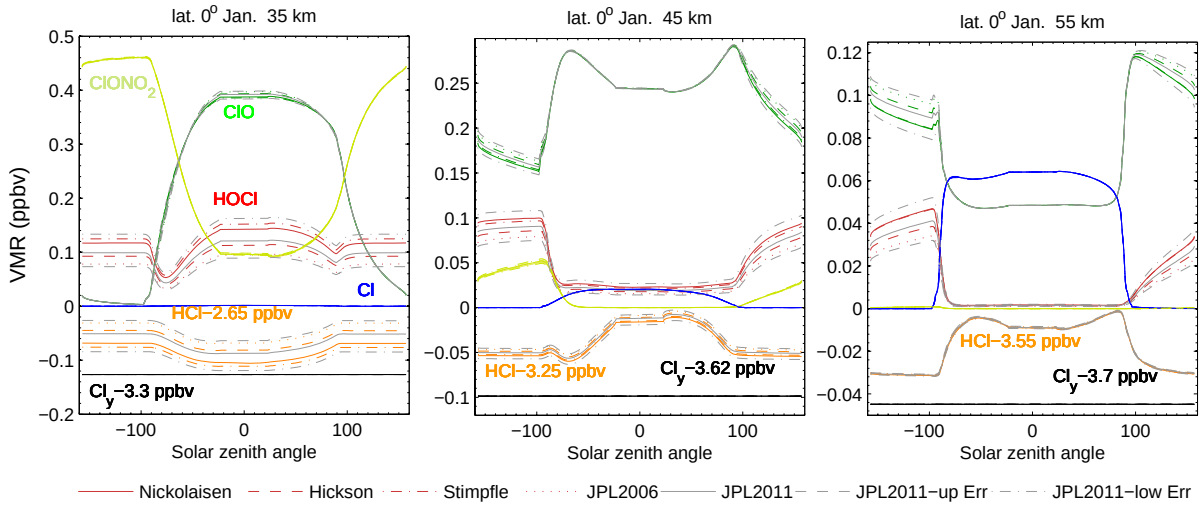

Fig. 7. Sensitivity of chlorine species in the model to different reaction rate constants for HOCl formation (k_1) at 35, 45 and 55 km (left, middle, and right) for solar conditions of 1 January at the equator. The different line styles represent model simulations using the reaction rates recommended by Nickolaisen et al. (2000), Hickson et al. (2007), Stimpfle et al. (1979) and JPL 2006 (Sander et al., 2006) (coloured lines, see legend). The simulations using the JPL 2011 (Sander et al., 2011) and the upper and the lower uncertainty limit of k_1 given by JPL 2011 are also shown (grey lines, see legend). The plots show volume mixing ratios plotted against solar zenith angle. HCl and Cl_y have been shifted for better visualisation, subtracted values are indicated in the individual plots.

impact on the HOCl diurnal variation in the lower mesosphere at 55 km, unlike in the stratosphere.

Figure 8 shows the observed and modelled diurnal variation of HOCl and ClO at the levels 35, 45 and 55 km after the offset shift. As before, the night-time measurements and model concentrations were subtracted from the corresponding measurements and model results in the MLS solar zenith angle range (between −130° and −160°) and then shifted respective to SMILES-R band B. MIPAS HOCl data were shifted using the MIPAS solar zenith angle range (140–150°) as reference. Note that the choice of the reference is not important if only the amplitude of the diurnal variation is considered. The errors of the measurements are not plotted for better visualisation of the model simulations. For this analysis, we carried out simulations for 1 January at latitude 0°, which gives almost the average of the model results for the period and location of our study. Observations of the diurnal variation of relevant species are taken over a longer time period of 6 months and an extended latitude band (20° N to 20° S). Uncertainties arising from different solar illumination at the different latitudes and times were previously discussed (see Figs. 3 and 6) and are shown in Fig. 8 as vertical error bars ("err-simulation"). These uncertainties are calculated in the solar zenith angle range of the MLS daytime observations (25–49°) for the shifted model results shown in Fig. 6. The effect of an 2 km uncertainty in the vertical resolution (vertical smoothing) on the model result is also indicated by error bars ("err-smooth") for each species.

As mentioned earlier, changes of k_1 in the lower mesosphere (55 km) lead only to changes of nighttime HOCl and ClO (shown in Fig. 7). The result for HOCl at 55 km is presented in the right plot in the top row of Fig. 8. As we have shifted the simulations and the observations to agree during nighttime in the MLS or MIPAS solar zenith angle ranges, the changes of HOCl occurring during nighttime are now visible at daytime. The SMILES observations fall in the range of the JPL 2011 errors for k_1. The MIPAS measurements are outside of this range. The difference between the model calculations at lower altitudes is less significant and roughly falls in the uncertainty range of the measurements (SMILES, MLS and MIPAS). As can be further inferred from the HOCl plot at 55 km, the best agreement between the model and the observations is obtained when using the upper limit of the JPL 2011 uncertainty range or the JPL 2006 recommendation for calculation of the reaction rate, whilst using the rate coefficients from Nickolaisen et al. (2000) and Stimpfle et al. (1979) give the poorest agreement. Tests showed that the value from the study of Hickson et al. (2007) and the JPL 2011 recommendation (Sander et al., 2011) can also be accommodated if the uncertainty arising from vertical smoothing and the error of the simulations arising from different assumptions of latitudes and months are considered.

The bottom row in Fig. 8 shows the amplitude of the diurnal variation of ClO together with the model calculations for the different k_1 values. At 55 km, daytime ClO and HOCl are partly converted to Cl and HCl and the day-night difference of ClO does not correspond to the day-night HOCl amplitude. The results of daytime simulations can therefore not clearly indicate which reaction rate leads to the best agreement between the model and the observations. The daytime

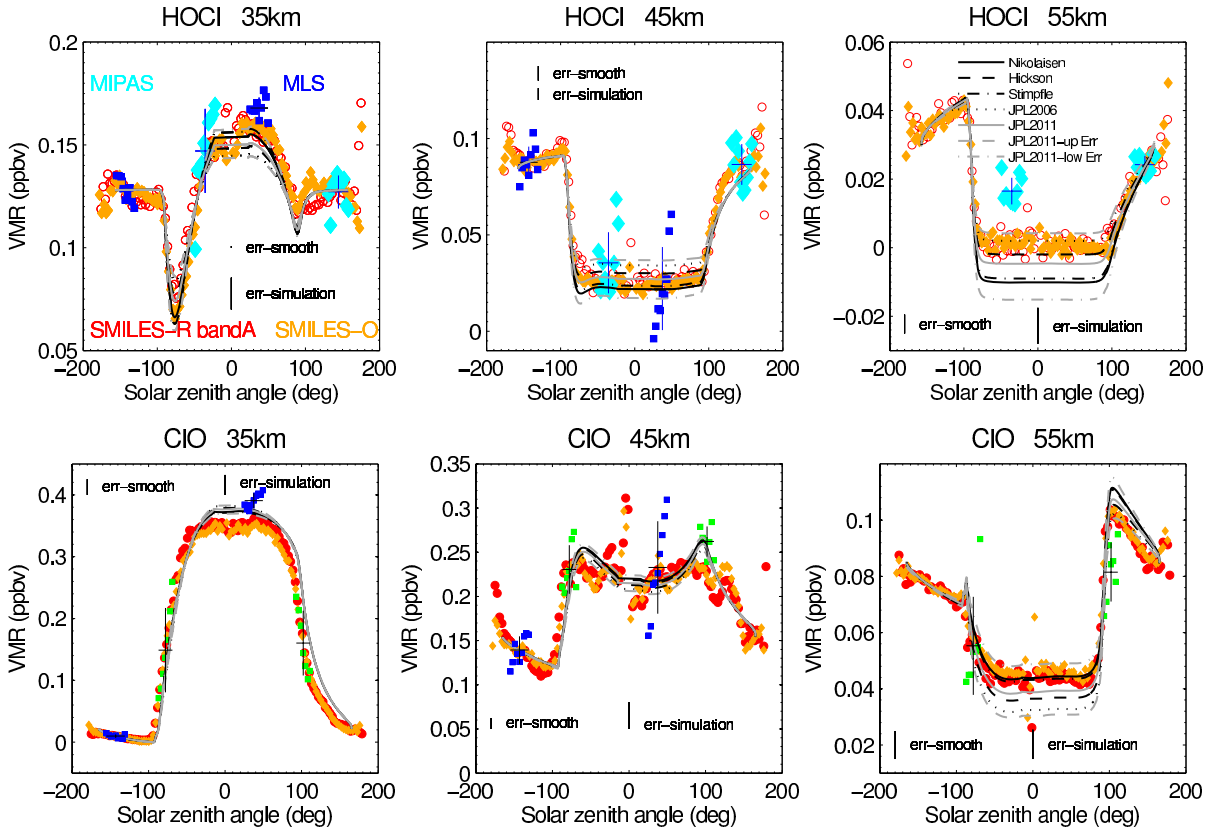

Fig. 8. Sensitivity of the model to different reaction rate constants for HOCl formation (k_1) at the altitudes of 35, 45 and 55 km (left, middle, and right) for solar conditions of 1 January at the equator. The black and grey coloured lines represent model simulations based on different recommendations for the reaction rate k_1 (see legend). Top: offset shifted observations and model results for HOCl. Bottom: same, but for ClO. The model has been vertically smoothed as indicated in Figs. 3 and 5. The total range of uncertainty arising from a 2 km change in vertical smoothing is shown as separate error bar (err-smooth) in each panel. The total range of model results obtained for different latitudes (20° S, Eq, 20° N) and months (November–April), derived from the offset corrected simulations shown in Fig. 5, is also indicated as vertical bar (err-simulations).

ClO measurements are thus irrelevant for this study and only the nighttime variations (slope in the range of 90° to 180°) should be considered. At this altitude the amplitude of the night-time variation of ClO, namely the difference of ClO between sunset (solar zenith angle 90°) and the reference period for offset-correction corresponding to the MLS nighttime observations (1.30 a.m. or solar zenith angle range of about −130° to −160°), is consistent with the model result obtained with k_1 within the range of the upper limit of the JPL 2011 (Sander et al., 2011) uncertainty range and the JPL 2006 recommendation (Sander et al., 2006). Given the smoothing and latitude-month uncertainties of the model calculations for ClO, k_1 values by Hickson et al. (2007) and JPL 2011 (Sander et al., 2011) can also be accepted. This is compatible with the results found for HOCl.

Our result contradicts the study of k_1 by Kovalenko et al. (2007) which has been done for lower altitudes (below 36 km) and is also not fully consistent with the results of von Clarmann et al. (2012), whose global data covered all seasons and a wide range of temperatures, but whose analysis was focused on altitudes below 45 km. The reaction rate k_1 is temperature dependent, so one may obtain different results at different altitudes. Note that the HOCl formation rate constants from JPL 2009 (Sander et al., 2009), assessed by von Clarmann et al. (2012), are identical to those in JPL 2011 (Sander et al., 2011). Our results are consistent with the quantitative analysis of k_1 by Kuribayashi et al. (2013).

5 Summary and conclusions

The diurnal variations of HOCl, ClO, HO_2 and HCl calculated with a 1-D chemical model were compared with observations of these species by three sub-millimetre instruments (Odin/SMR, Aura/MLS and SMILES) and two infrared spectrometers (SCISAT/ACE-FTS and ENVISAT/MIPAS) for the period of SMILES operations from November 2009 to April 2010, the latitude range of 20° N to 20° S, and three levels from the middle stratosphere to the lower mesosphere.

SMILES data and the model results are available for the whole range of solar zenith angles and thus allow to compare indirectly the MLS, SMR, MIPAS and ACE-FTS observations of short-lived species. This analysis includes new SMILES data, a new version of HO_2 measured by SMR and the latest version of MLS data.

The satellite observations of HOCl, ClO, HO_2 and HCl diurnal variations generally agree well both in quantity and in shape, considering the difficulties of comparisons between different sun-synchronous instruments. The modelled species generally reproduce very similar shapes of the diurnal variation as obtained from the satellite observations in the tropics at the altitudes 35, 45 and 55 km, where HOCl is mainly formed by the reaction of ClO and HO_2. The differences between the day and night data from model and satellites indicate almost similar diurnal variation amplitudes of the modelled and observed species. Exceptions are HOCl at 55 km and HO_2 at 45 and 55 km where the model (based on JPL 2011 and Stimpfle et al. (1979) for the HOCl formation reaction rate) calculates larger and lower amplitudes than the observations, respectively.

The absolute values of HOCl (in volume mixing ratio) from the simulations, MIPAS, and MLS agree with the range of SMILES observations at 35 km. The model and the observations agree well at 45 and 55 km, however MIPAS measures about three times higher HOCl at 45 km. Better agreement cannot be expected as the MIPAS data are taken from November 2003 to April 2004, when the overall chlorine level was higher. The enhanced HO_x chemistry during this period of relatively high solar activity compared to 2009/2010 could have led to more available HO_2. The difference between the day and night data from the model and satellites, namely the amplitude of the diurnal variation, indicate a very similar amplitude for the MLS, MIPAS and SMILES data as well as that of the model result at 35 and 45 km, but a slightly smaller amplitude for the MIPAS data compared with the model and the other instruments at 55 km.

The model ClO agrees well in absolute volume mixing ratio values with the observations at 35 and 45 km, however it calculates slightly higher ClO than the SMR and SMILES measurements at 55 km. After offset shift, the model amplitude of ClO between night and day agrees reasonably with that of the MLS and SMR at 35 and 45 km, but it is larger than that of SMR at 55 km. The SMILES amplitude of the ClO diurnal cycle agrees with that of the model at 45 and 55 km, but is slightly smaller at 35 km.

Odin/SMR HO_2 data have not been compared previously with other satellite observations and this study represents the first validation of SMR HO_2. Although SMR HO_2 data have been taken from a different time period than the other satellite observations, and despite the different solar activity during respective periods of observation, there is generally a good agreement between the SMR, MLS and SMILES observations and the simulations. Nevertheless, the SMR data after sunset are slightly higher than the model and the SMILES data at all altitudes. The absolute values of HO_2 agree best at 35 km, but at 45 and 55 km MLS and all SMILES datasets agree and are slightly higher than the model simulations. After offset correction, very similar amplitudes of the observations and the model are obtained for the 35 km level, however the model amplitude is smaller than that of all observations at higher altitudes.

The model and observations show a very weak diurnal variation of HCl at the three altitudes of 35, 45 and 55 km. There is a reasonable agreement between the observations at 35 km. The MLS and ACE-FTS measurements are consistent with the model HCl and are higher than the SMILES data at 45 and 55 km. This can be explained as the model is initialised with the Cl_y profile based on ACE-FTS and Odin/SMR measurements (Nassar et al., 2006) and was corrected for the decrease of Cl_y with time.

The best agreement between the model and observations is achieved when the reaction rate coefficient of the HOCl formation reaction (k_1) is calculated using the upper uncertainty limit of the JPL 2011 recommendations (Sander et al., 2011) or recommendations from JPL 2006 (Sander et al., 2006). Reaction rate constants by Hickson et al. (2007) and JPL 2011 (Sander et al., 2011) are within the uncertainty of the simulations and can also be accepted. Results from Stimpfle et al. (1979) and Nickolaisen et al. (2000) give the worst agreement with the observations. This result contradicts the study by Kovalenko et al. (2007), which was done for lower altitudes (below 36 km) and is also not fully consistent with the results of von Clarmann et al. (2012), whose global data covered all seasons but whose analysis was focused on altitudes below 45 km.

The good agreement of the model and observed diurnal cycles can be used in the future to correct long-term datasets differing in local time using scaling factors from model simulations to obtain realistic time series for trend analysis (e.g. Brohede et al., 2007; Jones et al., 2011a).

Acknowledgements. The retrievals of IMK/IAA were performed on the HP XC4000 of the Scientific Supercomputing Center (SSC) Karlsruhe under project grant MIPAS. IMK data analysis was supported by DLR under contract number 50EE0901. MIPAS level 1B data were provided by ESA. Odin is a Swedish-led satellite project funded jointly by Sweden (SNSB), Canada (CSA), Finland (TEKES), and France (CNES). Since 2007 the Odin project is supported by the third party mission programme of the European Space Agency (ESA). The JEM/SMILES mission is a joint project of the Japan Aerospace Exploration Agency (JAXA) and the National Institute of Information and Communications Technology (NICT). Work at the Jet Propulsion Laboratory, California Institute of Technology, was done under contract with the National Aeronautics and Space Administration.

Edited by: A. Richter

References

Abbatt, J. P. D. and Molina, M. J.: The heterogeneous reaction of HOCl + HCl → Cl_2 + H_2O on ice and nitric acid trihydrate: Reaction probabilities and stratospheric implications, Geophys. Res. Lett., 19, 461–464, 1992.

Baron, P., Dupuy, É., Urban, J., Murtagh, D. P., Eriksson, P., and Kasai, Y.: HO_2 measurements in the stratosphere and the mesosphere from the sub-millimetre limb sounder Odin/SMR, Int. J. Remote Sens., 30, 4195–4208, 2009.

Baron, P., Urban, J., Sagawa, H., Möller, J., Murtagh, D. P., Mendrok, J., Dupuy, E., Sato, T. O., Ochiai, S., Suzuki, K., Manabe, T., Nishibori, T., Kikuchi, K., Sato, R., Takayanagi, M., Murayama, Y., Shiotani, M., and Kasai, Y.: The Level 2 research product algorithms for the Superconducting Submillimeter-Wave Limb-Emission Sounder (SMILES), Atmos. Meas. Tech., 4, 2105–2124, doi:10.5194/amt-4-2105-2011, 2011.

Barret, B., Ricaud, P., Santee, M. L., Attié, J.-L., Urban, J., Le Flochmoën, É., Berthet, G., Murtagh, D., Eriksson, P., Jones, A., de La Noë, J., Dupuy, É., Froideveaux, L., Livesey, N. J., Waters, J. W., and Filipiak, M. J.: Intercomparisons of trace gases profiles from the Odin/SMR and Aura/MLS limb sounders, J. Geophys. Res., 111, D21302, doi:10.1029/2006JD007305, 2006.

Bernath, P. F., McElroy, C. T., Abrams, M. C., Boone, C. D., Butler, M., Camy-Peyret, C., Carleer, M., Clerbaux, C., Coheur, P.-F., Colin, R., DeCola, P., DeMaziére, M., Drummond, J. R., Dufour, D., Evans, W. F. J., Fast, H., Fussen, D., Gilbert, K., Jennings, D. E., Llewellyn, E. J., Lowe, R. P., Mahieu, E., McConnell, J. C., McHugh, M., McLeod, S. D., Michaud, R., Midwinter, C., Nassar, R., Nichitiu, F., Nowlan, C., Rinsland, C. P., Rochon, Y. J., Rowlands, N., Semeniuk, K., Simon, P., Skelton, R., Sloan, J. J., Soucy, M.-A., Strong, K., Tremblay, P., Turnbull, D., Walker, K. A., Walkty, I., Wardle, D. A., Wehrle, V., Zander, R., and Zou, J.: Atmospheric Chemistry Experiment (ACE): Mission overview, Geophys. Res. Lett., 32, L15S01, doi:10.1029/2005GL022386, 2005.

Boone, C. D., Nassar, R., Walker, K. A., Rochon, Y., McLeod, S. D., Rinsland, C. P., and Bernath, P. F.: Retrievals for the atmospheric chemistry experiment Fourier-transform spectrometer, Appl. Opt., 44, 7218–7231, doi:10.1364/AO.44.007218, 2005.

Brohede, S., McLinden, C. A., Berthet, G., Haley, C. S., Murtagh, D., and Sioris, C. E.: A stratospheric NO_2 climatology from Odin/OSIRIS limb-scatter measurements, Can. J. Phys., 85, 1253–1274, 2007.

Burrows, J. P. and Cox, R. A.: Kinetics of chlorine oxide radical reactions using modulated photolysis. Part 4. The reactions Cl+ Cl_2O → Cl_2+ ClO and ClO+ HO_2 products studied at 1 atm and 300 K, J. Chem. Soc., Faraday Trans. 1, 77, 2465–2479, 1981.

Chance, K. V., Johnson, D. G., and Traub, W. A.: Measurement of stratospheric HOCl: Concentration profiles, including diurnal variation, J. Geophys. Res., 94, 11059–11069, doi:10.1029/JD094iD08p11059, 1989.

Dupuy, É., Urban, J., Ricaud, P., Le Flochmoën, É., Lautié, N., Murtagh, D., de La Noë, J., El Amraoui, L., Eriksson, P., Forkman, P., Frisk, U., Jégou, F., Jiménez, C., and Olberg, M.: Stratomesospheric measurements of carbon monoxide with the Odin Sub-Millimetre Radiometer: Retrieval and first results, Geophys. Res. Lett., 31, L20101, doi:10.1029/2004GL020558, 2004.

Flaud, J. M., Piccolo, C., Carli, B., Perrin, A., Coudert, L. H., Teffo, J. L., and Brown, L. R.: Molecular line parameters for the MIPAS (Michelson Interferometer for Passive Atmospheric Sounding experiment, Atmos. Ocean. Opt., 16, 172–182, 2003.

Frisk, U., Hagström, M., Ala-Laurinaho, J., Andersson, S., Berges, J.-C., Chabaud, J.-P., Dahlgren, M., Emrich, A., Florén, H.-G., Florin, G., Fredrixon, M., Gaier, T., Haas, R., Hirvonen, T., Hjalmarsson, Å., Jakobsson, B., Jukkala, P., Kildal, P., Kollberg, E., Lassing, J., Lecacheux, A., Lehikoinen, P., Lehto, A., Mallat, J., Marty, C., Michet, D., Narbonne, J., Nexon, M., Olberg, M., Olofsson, O., Olofsson, G., Origné, A., Petersson, M., Piironen, P., Pons, R., Pouliquen, D., Ristocelli, I., Rosolen, C., Rouaix, G., Räisänen, A., Serra, G., Sjöberg, F., Stenmark, L., Torchinsky, S., Tuovinen, J., Ullberg, C., Vinterhav, E., Wadefalk, N., Zirath, H., Zimmermann, P., and Zimmermann, R.: The Odin satellite: I. Radiometer design and test, Astron. Astrophys., 402, 27–34, 2003.

Froidevaux, L., Livesey, N. J., Read, W. G., Salawitch, R. J., Waters, J. W., Drouin, B., MacKenzie, I. A., Pumphrey, H. C., Bernath, P., Boone, C., Nassar, R., Montzka, S., Elkins, J., Cunnold, D., and Waugh, D.: Temporal decrease in upper atmospheric chlorine, Geophys. Res. Lett., 33, L23812, doi:10.1029/2006GL027600, 2006.

Froidevaux, L., Jiang, Y. B., Lambert, A., Livesey, N. J., Read, W. G., Waters, J. W., Fuller, R. A., Marcy, T. P., Popp, P. J., Fahey, D. W., Gao, R. S., Jucks, K. W., Stachnik, R. A., Toon, G. C., Christensen, L. E., Webster, C. R., Bernath, P. F., Boone, C. D., Walker, K. A., Pumphrey, H. C., Harwood, R. S., Manney, G. L., Schwartz, M. J., Daffer, W. H., Drouin, B. J., Cofield, R. E., Cuddy, D. T., Jarnot, R. F., Knosp, B. W., Perun, V. S., Snyder, W. V., Stek, P. C., Thurstans, R. P., and Wagner, P. A.: Validation of Aura Microwave Limb Sounder HCl measurements, J. Geophys. Res., 113, D15S25, doi:10.1029/2007JD009025, 2008.

Hanson, D. R. and Ravishankara, A. R.: Investigation of the reactive and nonreactive processes involving $ClONO_2$ and HCl on water and nitric acid doped ice, J. Phys. Chem, 96, 2682–2691, 1992.

Hickson, K. M., Keyser, L. F., and Sander, S. P.: Temperature dependence of the HO_2+ ClO reaction. 2. Reaction kinetics using the discharge-flow resonance-fluorescence technique, J. Phys. Chem. A, 111, 8126–8138, 2007.

Johnson, D. G., Traub, W. A., Chance, K. V., Jucks, K. W., and Stachnik, R. A.: Estimating the abundance of ClO from simultaneous remote sensing measurements of HO_2, OH, and HOCl, Geophys. Res. Lett., 22, 1869–1871, 1995.

Jones, A., Urban, J., Murtagh, D. P., Sanchez, C., Walker, K. A., Livesey, N. J., Froidevaux, L., and Santee, M. L.: Analysis of HCl and ClO time series in the upper stratosphere using satellite datasets, Atmos. Chem. Phys., 11, 5321–5333, doi:10.5194/acp-11-5321-2011, 2011a.

Jones, A., Qin, G., Strong, K., Walker, K. A., McLinden, C. A., Toohey, M., Kerzenmacher, T., Bernath, P. F., and Boone, C. D.: A global inventory of stratospheric NO_y from ACE-FTS, J. Geophys. Res., 116, D17304, doi:10.1029/2010JD015465, 2011b.

Jonsson, A.: Modelling the middle atmosphere and its sensitivity to climate change, Ph.D. thesis, Stockholm University, 2006.

Jucks, K. W., Johnson, D. G., Chance, K. V., Traub, W. A., Margitan, J. J., Osterman, G. B., and Salawitch, R. J.: Observations of OH, HO_2, H_2O, and O_3 in the upper stratosphere: implications for photochemistry, Geophys. Res. Lett., 25, 3935–3938, 1998.

Kasai, Y., Sagawa, H., Kreyling, D., Suzuki, K., Dupuy, E., Sato, T. O., Mendrok, J., Baron, P., Nishibori, T., Mizobuchi, S., Kikuchi,

K., Manabe, T., Ozeki, H., Sugita, T., Fujiwara, M., Irimajiri, Y., Walker, K. A., Bernath, P. F., Boone, C., Stiller, G., von Clarmann, T., Orphal, J., Urban, J., Murtagh, D., Llewellyn, E. J., Degenstein, D., Bourassa, A. E., Lloyd, N. D., Froidevaux, L., Birk, M., Wagner, G., Schreier, F., Xu, J., Vogt, P., Trautmann, T., and Yasui, M.: Validation of stratospheric and mesospheric ozone observed by SMILES from International Space Station, Atmos. Meas. Tech. Discuss., 6, 2643–2720, doi:10.5194/amtd-6-2643-2013, 2013.

Kikuchi, K., Nishibori, T., Ochiai, S., Ozeki, H., Irimajiri, Y., Kasai, Y., Koike, M., Manabe, T., Mizukoshi, K., Murayama, Y., Nagahama, T., Sano, T., Sato, R., Seta, M., Takahashi, C., Takayanagi, M., Masuko, H., Inatani, J., Suzuki, M., and Shiotani, M.: Overview and early results of the Superconducting Submillimeter-Wave Limb-Emission Sounder (SMILES), J. Geophys. Res., 115, D23306, doi:10.1029/2010JD014379, 2010.

Knight, G. P., Beiderhase, T., Helleis, F., Moortgat, G. K., and Crowley, N. J.: Reaction of HO_2 with ClO: Flow tube studies of kinetics and product formation between 215 and 298 K, J. Phys. Chem. A, 104, 1674–1685, 2000.

Ko, M. K. W. and Sze, N. D.: Diurnal variation of ClO: Implications for the Stratospheric Chemistries of $ClONO_2$, HOCl, and HCl, J. Geophys. Res., 89, 11619–11632, 1984.

Koppers, G. A. and Murtagh, D. P.: Model studies of the influence of O_2 photodissociation parametrizations in the Schumann-Runge bands on ozone related photolysis on the upper atmosphere, Annales Geophysicae, 14, 68–79, 1996.

Kovalenko, L. J., Jucks, K. W., Salawitch, R. J., Toon, G. C., Blavier, J. F., Johnson, D. G., Kleinböhl, A., Livesey, N. J., Margitan, J. J., Pickett, H. M., Santee, M. L., Sen, B., Stachnik, R. A., and Waters, J. W.: Observed and modeled HOCl profiles in the midlatitude stratosphere: Implication for ozone loss, Geophys. Res. Lett., 34, L19801, doi:10.1029/2007GL031100, 2007.

Kuribayashi, K., Sagawa, H., Lehmann, R., Sato, T. O., and Kasai, Y.: Direct estimation of the rate constant of the reaction ClO + HO_2 $\rightarrow$ HOCl + O_2 from SMILES atmospheric observations, Atmos. Chem. Phys. Discuss., 13, 12797–12823, doi:10.5194/acpd-13-12797-2013, 2013.

Larsen, J. C., Rinsland, C. P., Goldman, A., Murcray, D. G., and Murcray, F. J.: Upper limits for stratospheric H_2O_2 and HOCl from high resolution balloon-borne infrared solar absorption spectra, Geophys. Res. Lett., 12, 663–666, 1985.

Leck, T. J., Cook, Jac-E. L., , and Birks, J. W.: Studies of reactions of importance in the stratosphere. III. Rate constant and products of the reaction between ClO and HO radicals at 298 K, J. Chem. Phys., 72, 2364, doi:10.1063/1.439484, 1980.

Livesey, N. J., Read, W. G., Froidevaux, L., Lambert, A., Manney, G. L., Pumphrey, H. C., Santee, M. L., Schwartz, M. J., Wang, S., Cofield, R. E., Cuddy, D. T., Fuller, R. A., Jarnot, R. F., Jiang, J. H., Knosp, B. W., Stek, P. C., Wagner, P. A., and Wu., D. L.: EOS MLS Level 2 Version 3.3 Quality Document, Tech. rep., Jet Propulsion Laboratory, California Institute of Technology, Pasadena, California, 91109-8099, http://mls.jpl.nasa.gov/data/datadocs.php, 2011.

Madronich, S.: The atmosphere and UV-B radiation at ground level, Environmental UV Photobiology, 1, 39, 1993.

Mahieu, E., Duchatelet, P., Demoulin, P., Walker, K. A., Dupuy, E., Froidevaux, L., Randall, C., Catoire, V., Strong, K., Boone, C. D., Bernath, P. F., Blavier, J.-F., Blumenstock, T., Coffey, M., De Mazière, M., Griffith, D., Hannigan, J., Hase, F., Jones, N., Jucks, K. W., Kagawa, A., Kasai, Y., Mebarki, Y., Mikuteit, S., Nassar, R., Notholt, J., Rinsland, C. P., Robert, C., Schrems, O., Senten, C., Smale, D., Taylor, J., Tétard, C., Toon, G. C., Warneke, T., Wood, S. W., Zander, R., and Servais, C.: Validation of ACE-FTS v2.2 measurements of HCl, HF, CCl_3F and CCl_2F_2 using space-, balloon- and ground-based instrument observations, Atmos. Chem. Phys., 8, 6199–6221, doi:10.5194/acp-8-6199-2008, 2008.

Meier, R. R., Anderson Jr., D., and Nicolet, M.: Radiation field in the troposphere and stratosphere from 240–1000 nm. I-General analysis, Planet. Space. Sci., 30, 923–933, doi:10.1016/0032-0633(82)90134-9, 1982.

Mitsuda, C., Suzuki, M., Iwata, Y., Manago, N., Naito, Y., Takahashi, C., Imai, K., Nishimoto, E., Hayashi, H., Shiotani, M., Sano, T., Takayanagi, M., and Taniguchi, H.: Current status of level 2 product of Superconducting Submillimeter-Wave Limb-Emission Sounder (SMILES), vol. 8176, p. 81760M, SPIE, doi:10.1117/12.898135, 2011.

Murtagh, D. P., Frisk, U., Merino, F., Ridal, M., Jonsson, A., Stegman, J., Witt, G., Eriksson, P., Jiménez, C., Mégie, G., de La Noë, J., Ricaud, P., Baron, P., Pardo, J. R., Hauchecorne, A., Llewellyn, E., Degenstein, D., Gattinger, R., Lloyd, N. D., Evans, W., McDade, I., Haley, C., Sioris, C., von Savigny, C., Solheim, B., McConnell, J., Strong, K., Richardson, E., Leppelmeier, G., Kyrölä, E., Auvinen, H., and Oikarinen, L.: An overview of the Odin atmospheric mission, Can. J. Phys., 80, 309–319, 2002.

Nassar, R., Bernath, P. F., Boone, C. D., Clerbaux, C., Coheur, P. F., Dufour, G., Froidevaux, L., Mahieu, E., McConnell, J. C., McLeod, S. D., Murtagh, D. P., Rinsland, C. P., Semeniuk, K., Skelton, R., Walker, K. A., and Zander, R.: A global inventory of stratospheric chlorine in 2004, J. Geophys. Res., 111, D22312, doi:10.1029/2006JD007073, 2006.

Nickolaisen, S. L., Roehl, C. M., Blakeley, L. K., Friedl, R. R., Joseph, S. F., Liu, R., and Sander, S. P.: Temperature Dependence of the HO_2 + ClO Reaction. 1. Reaction Kinetics by Pulsed Photolysis-Ultraviolet Absorption and ab Initio Studies of the Potential Surface, J. Phys. Chem. A, 104, 308–319, 2000.

Nicolet, M. and Kennes, R.: Aeronomic problems of the molecular oxygen photodissociation I. The O_2 Herzberg continuum., Planet, 34, 1043–1059, doi:10.1016/0032-0633(86)90015-2, 1986.

Pickett, H. M., Drouin, B. J., Canty, T., Salawitch, R. J., Fuller, R. A., Perun, V. S., Livesey, N. J., Waters, J. W., Stachnik, R. A., Sander, S. P., Traub, W. A., Jucks, K. W., and Minschwaner, K.: Validation of Aura Microwave limb sounder OH and HO_2 measurements, J. Geophys. Res., 113, D16S30, doi:10.1029/2007JD008775, 2008.

Raper, O. E., Farmer, C. B., Zander, R., and Park, J. H.: Infrared spectroscopic measurements of halogenated sink and reservoir gases in the stratosphere from the ATMOS Spacelab 3 mission, J. Geophys. Res., 92, 9851–9858, 1987.

Reimann, B. and Kaufman, F.: Rate constant of the reaction HO_2 + ClO $\rightarrow$ HOCl+ O, J. Chem. Phys., 69, 2925, doi:10.1063/1.436850, 1978.

Ricaud, P., Chipperfield, M. P., Waters, J. W., Russell III, J. M., and Roche, A. E.: Temporal evolution of chlorine monoxide in the middle stratosphere, J. Geophys. Res., 105, 4459–4469, 2000.

Sagawa, H., Sato, T. O., Baron, P., Dupuy, E., Livesey, N., Urban, J., von Clarmann, T., de Lange, A., Wetzel, G., Kagawa, A., Murtagh, D. P., and Kasai, Y.: Comparison of SMILES ClO profiles with other satellite and balloon-based measurements, Atmos. Meas. Tech. Discuss., 6, 613–663, doi:10.5194/amtd-6-613-2013, 2013.

Sander, S. P., Friedl, R. R., Barker, J. R., Golden, D. M., Kurylo, M. J., Wine, P. H., Abbatt, J. P. D., Burkholder, J. B., Kolb, C. E., Moortgat, G. K., Huie, R. E., and Orkin, V. L.: Chemical kinetics and photochemical data for use in atmospheric studies, Tech. rep., JPL, evaluation number 15, JPL Publ., 06-2, 2006.

Sander, S. P., Friedl, R. R., Barker, J. R., Golden, D. M., Kurylo, M. J., Wine, P. H., Abbatt, J. P. D., Burkholder, J. B., Kolb, C. E., Moortgat, G. K., Huie, R. E., and Orkin, V. L.: Chemical kinetics and photochemical data for use in stmospheric Studies: supplement to Evaluation 15: update of key reactions, Tech. rep., JPL, evaluation number 16, JPL Publ., 09-31, 2009.

Sander, S. P., Friedl, R. R., Barker, J. R., Golden, D. M., Burkholder, J. B., Kolb, C. E., Kurylo, M. J., Moortgat, G. K., Wine, P. H., Abbatt, J. P. D., Huie, R. E., and Orkin, V. L.: Chemical kinetics and photochemical data for use in atmospheric studies, Tech. rep., JPL, evaluation number 17, JPL Publ., 10-6, 2011.

Santee, M. L., Lambert, A., Read, W. G., Livesey, N. J., Coeld, R. E., Cuddy, D. T., Daffer, W. H., Drouin, B. J., Froidevaux, L., Fuller, R. A., Jarnot, R. F., Knosp, B. W., Manney, G. L., Perun, V. S., Snyder, W. V., Stek, P. C., Thurstans, R. P., Wagner, P. A., Waters, J., Conner, B., Urban, J., Murtagh, D. P., Ricaud, P., Barret, B., Kleinböhl, A., Kuttippurath, J., Küllmann, H., Toon, G. C., and Stachnik, R. A.: Validation of the Aura Microwave Limb Sounder ClO Measurements, J. Geophys. R., 113, D15S22, doi:10.1029/2007JD008762, 2008.

Sato, T. O., Sagawa, H., Kreyling, D., Manabe, T., Ochiai, S., Kikuchi, K., Baron, P., Mendrok, J., Urban, J., Murtagh, D., Yasui, M., and Kasai, Y.: Strato-mesospheric ClO observations by SMILES: error analysis and diurnal variation, Atmos. Meas. Tech., 5, 2809–2825, doi:10.5194/amt-5-2809-2012, 2012.

Shampine, L. F. and Reichelt, M. W.: The Matlab ODE suite, SIAM J. Sci. Comput., 18, 1–22, 1997.

Stimpfle, R. M., Perry, R. A., and Howard, C. J.: Temperature dependence of the reaction of ClO and HO_2 radicals., J. Chem. Phys., 71, 5183, 1979.

Takahashi, C., Ochiai, S., and Suzuki, M.: Operational retrieval algorithms for JEM/SMILES level 2 data processing system., J. Quant. Spectrosc. Ra. Transfer, 111, 160–173, 2010.

Takahashi, C., Suzuki, M., Mitsuda, C., Ochiai, S., Manago, N., Hayashi, H., Iwata, Y., Imai, K., Sano, T., Takayanagi, M., and Shiotani, M.: Capability for ozone high-precision retrieval on JEM/SMILES observation, Adv. Space Res., 48, 1076–1085, 2011.

Toon, G. C., Farmer, C. B., Schaper, P. W., Lowes, L. L., and Norton, R. H.: Composition measurements of the 1989 Arctic winter stratosphere by airborne infrared solar absorption spectroscopy, J. Geophys. Res., 97, 7939–7961, 1992.

Urban, J., Lautie, N., Le Flochmoën, E., Jiménez, C., Eriksson, P., de La Noë, J., Dupuy, É., Ekström, M., EL Amraoui, L., Frisk, U., Murtagh, D., Olberg, M., and Ricaud, P.: Odin/SMR limb observations of stratospheric trace gases: Level 2 processing of ClO, N_2O, HNO_3, and O_3, J. Geophys. Res., 110, D114307, doi:10.1029/2004JD005741, 2005.

Urban, J., Murtagh, D., Lautié, N., Barret, B., Dupuy, É., de La Noë, J., Eriksson, P., Frisk, U., Jones, A., Le Flochmoën, E., Olberg, M., Piccolo, C., Ricaud, P., and Rösevall, J.: Odin/SMR Limb Observations of Trace Gases in the Polar Lower Stratosphere during 2004-2005, in: Proc. ESA First Atmospheric Science Conference, 8-12 May 2006, Frascati, Italy, edited by: Lacoste, H., vol. ESA-SP-628 of European Space Agency publications, European Space Agency, ISBN-92-9092-939-1, ISSN-1609-042X, 2006.

von Clarmann, T., Wetzel, G., Oelhaf, H., Friedl-Vallon, F., Linden, A., Maucher, G., Seefeldner, M., Trieschmann, O., and Lefevre, F.: $ClONO_2$ vertical profile and estimated mixing ratios of ClO and HOCl in winter Arctic stratosphere from Michelson interferometer for passive atmospheric sounding limb emission spectra, J. Geophys. Res., 102, 16157–16168, 1997.

von Clarmann, T., Glatthor, N., Grabowski, U., Höpfner, M., Kellmann, S., Linden, A., Tsidu, G., Milz, M., Steck, T., Stiller, G. P., Fischer, H., and Funke, B.: Global stratospheric HOCl distributions retrieved from infrared limb emission spectra recorded by the Michelson Interferometer for Passive Atmospheric Sounding (MIPAS), J. Geophys. Res., 111, D05311, doi:10.1029/2005JD005939, 2006.

von Clarmann, T., Glatthor, N., Ruhnke, R., Stiller, G. P., Kirner, O., Reddmann, T., Höpfner, M., Kellmann, S., Kouker, W., Linden, A., and Funke, B.: HOCl chemistry in the Antarctic Stratospheric Vortex 2002, as observed with the Michelson Interferometer for Passive Atmospheric Sounding (MIPAS), Atmos. Chem. Phys., 9, 1817–1829, doi:10.5194/acp-9-1817-2009, 2009.

von Clarmann, T., Funke, B., Glatthor, N., Kellmann, S., Kiefer, M., Kirner, O., Sinnhuber, B.-M., and Stiller, G. P.: The MIPAS HOCl climatology, Atmos. Chem. Phys., 12, 1965–1977, doi:10.5194/acp-12-1965-2012, 2012.

Wang, S., Li, K., Pongetti, T. J., Sander, S. P., Yung, Y. L., Liang, M., Livesey, N. J., Santee, M. L., Harder, J. W., Snow, M., and Mills, F. P.: Mid-latitude Atmospheric OH Response to the Most Recent 11-year Solar Cycle., P. Natl. Acad. Sci., 110, 2023–2028, doi:10.1073/pnas.1117790110, 2013.

Waters, J. W., Froidevaux, L., Harwood, R. S., Jarnot, R. F., Pickett, H. M., Read, W. G., Siegel, P. H., Cofield, R. E., Filipiak, M. J., Flower, D. A., Holden, J. R., Lau, G. K., Livesey, N. J., Manney, G. L., Pumphrey, H. C., Santee, M. L., Wu, D. L., Cuddy, D. T., Lay, R. R., Loo, M. S., Perun, V. S., Schwartz, M. J., Stek, P. C., Thurstans, R. P., Boyles, M. A., Chandra, K. M., Chavez, M. C., Chen, G.-S., Chudasama, B. V., Dodge, R., Fuller, R. A., Girard, M. A., Jiang, J. H., Jiang, Y., Knosp, B. W., LaBelle, R. C., Lam, J. C., Lee, K. A., Miller, D., Oswald, J. E., Patel, N. C., Pukala, D. M., Quintero, O., Scaff, D. M., Van Snyder, W., Tope, M. C., Wagner, P. A., and Walch, M. J.: The Earth Observing System Microwave Limb Sounder (EOS MLS) on the Aura satellite, IEEE T. Geosci. Remote., 44, 1075–1092, 2006.

WMO: Atmospheric Ozone 1985, WMO Global Ozone Research and Monitoring Project, Report No. 16, Geneva, 1986.

WMO: Scientific Assesment of Ozone Depletion 2010, WMO Global Ozone Research and Monitoring Project, Report No. 16, Geneva, 2010.

Wrotny, J. E., Nedoluha, G. E., Boone, C., Stiller, G. P., and McCormack, J. P.: Total hydrogen budget of the equatorial upper stratosphere, J. Geophys. Res.-Atmos., 115, D04302, doi:10.1029/2009JD012135, 2010.